

Neuroimaging Cerebrovascular Function and Diffuse Axonal Injury after Traumatic  
Brain Injury and Response to Sildenafil Treatment

by

Angela M. Pronger

Dissertation submitted to the Faculty of the  
Neuroscience Graduate Program  
Uniformed Services University of the Health Sciences  
In partial fulfillment of the requirements for the degree of  
Doctor of Philosophy 2016



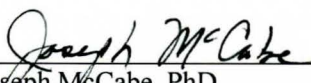
APPROVAL OF THE DOCTORAL DISSERTATION IN THE NEUROSCIENCE GRADUATE PROGRAM

Title of Dissertation: "Neuroimaging Cerebrovascular Function and Diffuse Axonal Injury after Traumatic Brain Injury and Response to Sildenafil Treatment"


Name of Candidate: Angela M. Pronger  
Doctor of Philosophy  
March 17, 2016

DISSERTATION AND ABSTRACT APPROVED:

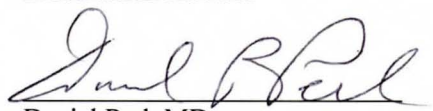
DATE:

  
Joseph McCabe, PhD  
DEPARTMENT OF ANATOMY, PHYSIOLOGY & GENETICS  
Committee Chairperson

4/5/16

  
Ramon Diaz-Arrastia, MD, PhD  
DEPARTMENT OF NEUROLOGY  
Dissertation Advisor

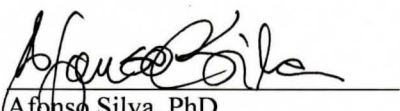
3/17/2016

  
Daniel Perl, MD  
DEPARTMENT OF PATHOLOGY  
Committee Member

3/17/16

  
LCDR Scott R. Jones, PhD  
DEPARTMENT OF RADIOLOGY & RADIOLOGICAL SCIENCES  
Committee Member

3/17/16

  
Afonso Silva, PhD  
NATIONAL INSTITUTE OF NEUROLOGICAL DISORDERS & STROKE, CEREBRAL  
MICROCIRCULATION UNIT  
Committee Member

3/17/16

## **ACKNOWLEDGMENTS**

I came to the Uniformed Services University of the Health Sciences in 2010 with a curiosity to study traumatic brain injury and a yearning to better understand translational medicine. I had hopes of developing as a neuroscientist and to become a physician, though I wasn't sure exactly where I was going, let alone how. Six years and several more grey hairs later, a new horizon has finally come to view. Numerous very distinguished people have guided me along the way; I could not have done it without them.

Dr. Joe McCabe, I am extremely grateful for you taking me under your wing from the start and for Chairing my Dissertation Committee. Dr. McCabe introduced me to the world of traumatic brain injury and it was in his lab I familiarized myself with many of the basics of the research. He has seen me through perils unnumbered and has provided invaluable direction.

Dr. Afonso Silva, thank you for opening your door to an aspiring neuroscientist. Meetings with Dr. Silva challenged me to think critically about several aspects in experimental design. He was always available to answer my questions about neuroimaging, and his lab gave tremendous support both to USUHS Translational Imaging Facility and me.

Dr. Dan Perl, you have been an excellent role model to me during my time at Twinbrook, and I truly appreciate your expertise in neuropathology for my project. I always admired Dr. Perl's frank input during lab meetings. On top of running his lab, leading the CNRM Brain Tissue Repository, etc., I was honored that he would still set aside time to examine slides of the rat brains and offer guidance.

LCDR Scott Jones, thank you for looking out for me and for your support throughout the evolution in the project. LCDR Jones guided my planning for the project and was often the voice of reason. I am very appreciative of his direction in setting goals and figuring out the means to accomplish them.

Dr. Ramon Diaz-Arrastia, I am deeply thankful for your guidance through “the swamp” of graduate school and honored to have been given the opportunity to work in your lab with you as my Major Advisor. I could not have found a better mentor or a more perfect match in a lab. What other PI would agree to meet each Saturday morning to talk about science over coffee and bagels? Dr. D-A said it was the best part of his weekend, and I agreed. He does whatever is necessary to do what needs to be done. Time and again I am impressed how he can not only describe the latest finding in a given field, but the history of its development, the scientist who discovered it, and can get you on the phone with him in five minutes. Dr. D-A’s mentorship played a fundamental role in my development as a scientist. He has been a truly remarkable role model; I would be extremely fortunate to some day have an RDA lab of my own.

The RDA lab has provided great assistance in the project, especially Dr. Margalit Haber who provided technical and emotional support in histologic and MRI data analysis, Drs. Bao-Xi Qu and Yale Gong who assisted monitoring animals and analyzing behavioral data, and Emily Spessert who assisted in MRI data processing. Dr. Frank Amyot, thank you so much for your technical expertise in data processing throughout the study. Dr. Kim Kenney, Carol Moore, and all of Camp RDA, thank you for your assistance through the project and unwavering support!

To all of the Leonessa lab, I could not possibly thank you enough for your contributions to this project. Dr. Leonessa, I am incredibly grateful for being able to complete studies in your lab. Erin Murphy, Drs. Krisztian Kovacs and Hongna Pan, thank you for your dedication in training me, and generous assistance with behavioral studies. Erin, I am particularly indebted to you for the countless hours you invested in helping me during this project.

To the Translational Imaging Facility, I thank you for bearing the heavy load with me. Drs. Asamoah Bosomtwi and Alex Korotcov, I thank you profusely for your immense patience as well as your devotion to this project and my professional development. Over the seemingly infinite hours of scanning, I found in both of you an incredible teacher and cherished friend.

To the other members of my Qualifying Committee, Drs. Sue Bausch, Brian Cox, Zygmunt Galdzicki, I thank you for always having an open door and for challenging my knowledge and critical thinking. This committee helped me grow significantly as a scientist, and everyone's input considerably molded the design of this project.

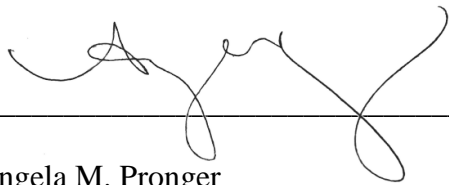
Finally, I would like to thank my professors, the graduate students, medical students, lab techs, friends, family, Herbert, and Golgi for the unyielding support and encouragement over the arduous and highly rewarding journey. Thank you for lending a luer lock, training me to intubate rats, sharing that cup of coffee, and always being there. Your generosity will be always remembered.

## DEDICATION

My siblings and I were recently talking about childhood memories of visiting museums in the city. When one of us mentioned the Field Museum, my father commented, “Angela, you were never happy going there.” I was surprised by this, as I regarded it as one of my favorites. He explained that I was not content in looking at the fossils under the glass, I wanted to find them on my own. He would drive my siblings and I to a quarry and we would return home with buckets of rocks, secrets of hundreds of millions of years of life we explored together. We naturally learned to ask how and why, and my parents somehow had the patience to come up with an answer when we asked. My mother always told us to ask a good question before we left for school. We enjoyed solving puzzles together. She would say it was okay if my brother and I wanted to take apart the old gas chromatograph- mass spectrometer in the garage for fun. My parents entertained our crazy plans to construct perpetual motion machines, taking us to the hardware store and never telling us our ideas were impossible. I dedicate this work to them.

## **COPYRIGHT STATEMENT**

The author hereby certifies that the use of any copyrighted material in the dissertation manuscript entitled: *Neuroimaging Cerebrovascular Function and Diffuse Axonal Injury after Traumatic Brain Injury and Response to Sildenafil Treatment* is appropriately acknowledged and, beyond brief excerpts, is with the permission of the copyright owner.



---

Angela M. Pronger

May 20, 2016

## **DISCLAIMER**

The views presented here are those of the author and are not to be construed as official or reflecting the views of the Uniformed Services University of the Health Sciences, the Department of Defense or the U.S. Government.

## **ABSTRACT**

Neuroimaging Cerebrovascular Function and Diffuse Axonal Injury after Traumatic Brain Injury and Response to Sildenafil Treatment:

Angela M. Pronger, B.S., 2016

Thesis directed by: Ramon Diaz-Arrastia, MD/PhD, Director of Clinical Research, Center for Neuroscience and Regenerative Medicine, Professor of Neurology, Uniformed Services University of the Health Sciences

Damage to the cerebral microvasculature and diffuse axonal injury (DAI) are two well recognized endophenotypes of traumatic brain injury (TBI) which significantly contribute to neuropsychological sequelae (40; 61; 110). Patients who have suffered mild TBI show acute disruptions in cerebrovascular reactivity (73) and chronic regional deficits in cerebral blood flow (CBF) that are concordant with neuropsychiatric localization (18). Furthermore, compelling evidence indicates that enhancing angiogenesis may attenuate secondary injury and improve functional recovery (21; 77; 121; 122; 136). Although diffuse axonal injury has similarly been linked to neurologic outcome (70), the relationship of microvascular disease and axonal injury after TBI remains unknown.



The present study establishes a method to efficiently and non-invasively quantify traumatic cerebral microvascular injury after TBI and response to therapeutic intervention, using sildenafil as a model. Young adult male rats were assessed over a 30-day period following moderate fluid percussion injury through multimodal magnetic resonance imaging. Cerebrovascular reactivity to hypercapnia was measured using arterial spin labeling. Diffusion tensor imaging was employed to assess microstructural alterations, including axonal injury. Neurobehavioral outcome was assessed by the Neurological Severity Score, Morris Water Maze, Rotarod, and Open Field Test. Animals were euthanized 30 days after injury for histological measures of astrogliosis (GFAP), microgliosis (Iba-1) and vascular recovery (RECA-1). The effectiveness of sildenafil (Viagra, Revatio) as a cytoprotective treatment was also evaluated using these methods.

Regional deficits in cerebrovascular function were concordant with regions of increased astrogliosis and microglial activation (GFAP and Iba-1 increased in auditory cortex, each  $p < 0.001$ ). The CBF deficits at rest and during hypercapnia that were observed in injured animals were not seen for the injured group that received sildenafil treatment, though a statistically significant main effect of treatment was not detected. Sildenafil treated animals also showed a non-statistically significant trend toward ameliorated neurologic function following injury. Diffusion imaging revealed significant microstructural changes following injury, many of which were reversed with sildenafil treatment. After fluid percussion injury, mean diffusivity (MD) increased in the medial and lateral external capsule ( $p < 0.0001$ ) and the day 1 increase reversed with sildenafil treatment ( $p = 0.0024$  medial segment,  $p = 0.0040$  lateral segment). MD also increased in

the medial and lateral cortex ( $p<0.0001$ ), and the day 1 increase similarly reversed with sildenafil treatment in the medial cortex ( $p=0.0028$ ). Fractional anisotropy (FA) decreased in the lateral external capsule, and FA on day 30 was increased with sildenafil treatment ( $p=0.0275$ ). Axial diffusivity (AD) demonstrated an early increase on day 1, and decrease by day 30 in the medial and lateral external capsule ( $p<0.0001$ ). Radial diffusivity (RD) increased on day 1 in the lateral external capsule ( $p<0.0001$ ), and sildenafil significantly decreased RD on day 1 ( $p<0.0001$ ). However, a direct correlation between CBF either during rest or hypercapnia did not appear to correlate with DTI scalars.

In summary, this study establishes a non-invasive imaging biomarker for the pathoanatomic classification of TBI focusing on two mechanisms, and demonstrates assessment of mechanism-specific therapy. Our results suggest that sildenafil may improve functional recovery after TBI by enhancing microvascular recovery and attenuating diffusion abnormalities. Further research is indicated to investigate the relationship between cerebrovascular function and axonal injury to facilitate identification of targets for mechanism specific therapies.

## TABLE OF CONTENTS

LIST OF TABLES .....	xii
LIST OF FIGURES .....	xiii
LIST OF ABBREVIATIONS.....	xiv
CHAPTER 1: INTRODUCTION .....	1
CHAPTER 2: BACKGROUND .....	5
Pathophysiology of Cerebral Microvascular Injury.....	5
Pathology of Microvascular Injury .....	5
Chronic Traumatic Encephalopathy .....	6
Imaging Traumatic Cerebral Vascular Injury: Clinical Studies .....	7
Candidate Pro-Angiogenic Treatments.....	10
Diffuse Axonal Injury.....	12
White Matter Damage and Vascular Dysfunction.....	12
Effect of Vascular Injury and White Matter Lesions on Cognitive Function.....	13
White Matter Damage in TBI .....	14
Animal Model .....	17
Animal Selection.....	17
Fluid Percussion Injury .....	17
Defining Sham .....	18
CHAPTER 3: SPECIFIC AIMS .....	19
CHAPTER 4: METHODOLOGIES .....	21
Study Paradigm.....	21
Surgical Procedures .....	22
MRI methods .....	22
Arterial Spin Labeling (ASL) .....	24
Diffusion Tensor Imaging.....	24
Data Analysis .....	25
Neurobehavioral testing.....	25
Rotarod.....	26
Morris Water Maze .....	27
Open Field Testing.....	28
Histology.....	28
CHAPTER 5: RESULTS.....	31
Animals Excluded from Study.....	31

Aims 1 & 2: A Non-Invasive Model to Assess Cerebrovascular Deficits and Response to Therapeutic Intervention.....	31
Arterial Spin Labeling Detects Deficits in Cerebrovascular Function after TBI.....	31
Arterial Spin Labeling Assesses Sildenafil Effect After TBI .....	35
Neurobehavioral Assessment after FPI.....	38
Neurologic Severity Score and Neurologic Severity Score-Revised.....	38
Open Field.....	39
Rotorod .....	40
Water Maze .....	40
Histologic Correlates .....	42
Aim 3: The Relation Between Cerebrovascular and Axonal Injury .....	46
Chapter 6: Discussion .....	66
Conclusion .....	71
Appendix I .....	73
Neurologic Severity Score (NSS) .....	73
Neurobehavioral Scale .....	75
NIH Stroke Severity Score.....	75
REFERENCES .....	76

## LIST OF TABLES

Table 1. DTI findings in Vascular Disease and after TBI. ....	16
Table 2. Summary of Histologic and MRI Findings in Right Auditory Cortex after TBI.....	59
Table 3. Summary of Histologic and MRI Findings in Right External Capsule after TBI. ....	60
Table 4. Correlation of Resting CBF and DTI Parameters of Injured Grey Matter. ....	62
Table 5. Correlation of Resting CBF in Injured Cortex and DTI Parameters of Adjacent White Matter. ....	64

## LIST OF FIGURES

Figure 1. Study Paradigm. ....	21
Figure 2. Effect of Hypercapnia on CBF. ....	32
Figure 3. Resting Cerebral Blood Flow after Moderate Fluid Percussion Injury. ....	32
Figure 4. Cerebral Blood Flow with Hypercapnia after Moderate Fluid Percussion Injury. ....	33
Figure 5. Cerebrovascular Reactivity after Moderate Fluid Percussion Injury and Vehicle Injection. ....	34
Figure 6. Min to Max Box and Whiskers Plot of CVR Values. ....	34
Figure 7. CVR Values Normalized to Mean of Contralateral ROI. ....	35
Figure 8. Resting Cerebral Blood Flow after Moderate Fluid Percussion Injury and Sildenafil Treatment. ....	36
Figure 9. Cerebral Blood Flow with Hypercapnia after Moderate Fluid Percussion Injury and Sildenafil Treatment. ....	36
Figure 10. Effect of Sildenafil on Resting Cerebral Blood Flow in Right Auditory Cortex after TBI. ....	37
Figure 11. Effect of Sildenafil on Cerebral Blood Flow during Hypercapnia in Right Auditory Cortex after TBI. ....	37
Figure 12. Temporal Profile of Neurologic Severity Score (NSS). ....	38
Figure 13. Temporal Profile of Neurologic Severity Score Revised (NSS-R) for the Treated and Control Groups. ....	39
Figure 14. Time Spent in Center by Open Field Test. ....	40
Figure 15. Water Maze Escape Latency during Training. ....	41
Figure 16. Water Maze Escape Latency across Training Days and Test Day. ....	41
Figure 17. Representative Images of GFAP and Iba-1 Immunoreactivity. ....	43
Figure 18. Representative Images of Iba-1 Morphology. ....	44
Figure 19. Increased GFAP Immunoreactivity after Injury. ....	44
Figure 20. Increased Iba-1 Immunoreactivity after Injury. ....	45
Figure 21. RECA-1 Immunolabeling of Vasculature 1 Month after Injury. ....	46
Figure 22. Regions of Interest Included in Diffusion Tensor Imaging Analysis. ....	47
Figure 23. Mean Diffusivity of White Matter. ....	48
Figure 24. Mean Diffusivity of Medial External Capsule. ....	49
Figure 25. Mean Diffusivity of Lateral External Capsule. ....	49
Figure 26. Mean Diffusivity of Grey Matter. ....	50
Figure 27. Mean Diffusivity of Medial Cortex. ....	51
Figure 28. Mean Diffusivity of Lateral Cortex. ....	51
Figure 29. Fractional Anisotropy in White Matter. ....	52
Figure 30. Fractional Anisotropy of Lateral External Capsule. ....	53
Figure 31. Axial Diffusivity in White Matter. ....	54
Figure 32. Radial Diffusivity in White Matter. ....	55
Figure 33. Radial Diffusivity of Lateral External Capsule. ....	56
Figure 34. Radial Diffusivity in Grey Matter. ....	57
Figure 35. Radial Diffusivity of Right Medial Cortex. ....	57
Figure 36. Radial Diffusivity of Right Lateral Cortex. ....	58

## LIST OF ABBREVIATIONS

2D: two-dimensional

ABC: Avidin-Biotin Complex

AD: Axial Diffusivity

ANOVA: Analysis of Variance

ASL: Arterial Spin Labeling

atm: atmospheres

Aud Cx: Auditory Cortex

$\beta$ -APP: Amyloid Beta Precursor Protein

BBB: Blood-Brain Barrier

BFV: Blood Flow Velocity

*bid*: twice daily

BOLD: Blood Oxygen Level Dependent

CADASIL: Cerebral Autosomal Dominant Arteriopathy with Subcortical Infarcts and  
Leukoencephalopathy

CASL: Continuous Arterial Spin Labeling

CBF: Cerebral Blood Flow

CCI: Controlled Cortical Impact

CO<sub>2</sub>: carbon dioxide

CT: Computerized Tomography

CTE: Chronic Traumatic Encephalopathy

CVR: Cerebrovascular Reactivity

d: day (post injury)

DAI: Diffuse Axonal Injury

DEtA/NONOate: (Z)-1-[2-(2-aminoethyl)-*N*-(2-ammonioethyl)amino]diazen-1-ium-1,2-diolate

DF: Degrees of Freedom

dHb: deoxyhemoglobin

DTI: Diffusion Tensor Imaging

Ext Cap: External Capsule

FDA: United States Food and Drug Administration

FIJI: Fiji Is Just ImageJ

FLAIR: Fluid-Attenuated Inversion Recovery

FA: Fractional Anisotropy

FDA: United States Food and Drug Administration

FDR: False Discovery Rate

FOV: field of view

FPI: Fluid Percussion Injury

g: grams

GCS: Glasgow Coma Scale

GFAP: Glial Fibrillary Acidic Protein

GRE: Gradient Echo

H<sub>2</sub>O<sub>2</sub>: hydrogen peroxide

hr: hours

Iba-1: Ionized calcium-Binding Adapter molecule-1

*ip*: intraperitoneal



Kg: Kilograms

LPM: Liters per Minute

M: Molar

MA: Medical Air

MCA<sub>v</sub>: blood flow Velocity in the Middle Cerebral Artery

mg: milligrams

min: minutes

MIPAV: Medical Image Processing, Analysis, and Visualization

MR: Magnetic Resonance

MRI: Magnetic Resonance Imaging

MD: Mean Diffusivity

mL: milliliters

msec: milliseconds

mTBI: mild Traumatic Brain Injury

N<sub>2</sub>: Nitrogen gas

NFT: Neurofibrillary Tangle

NGS: Normal Goat Serum

NIBIB: National Institute of Biomedical Imaging and Bioengineering

NICHD: National Institute of Child Health and Human Development

NIH: National Institutes of Health

NINDS: National Institute of Neurological Disorders and Stroke

NIRS: Near InfraRed Spectroscopy

NO: Nitric Oxide

NSS: Neurological Severity Score

NSS-R: Neurological Severity Score-Revised

NVU: Neurovascular Unit

O<sub>2</sub>: Oxygen gas

p: p-value

PBS: Phosphate Buffered Saline

PDW: Proton Density Weighted

PET: Positron Emission Tomography

PFA: paraformaldehyde

PTA: Post-Traumatic Amnesia

rCBF: regional Cerebral Blood Flow

RD: Radial Diffusivity

RECA-1: Rat Endothelial Cell Antigen-1

ROI: Region of Interest

RPM: Rotations per Minute

Rt: Right

SD: Sprague-Dawley

sec: seconds

SE: Standard Error

SEM: Standard Error of the Mean

SNAP: S-nitroso-N-acetylpenicillamine

SNP: Sodium Nitroprusside

SPECT: Single Photon Emission Computed Tomography

SpO<sub>2</sub>: saturation of peripheral oxygen

SWI: Susceptibility Weighted Imaging

T: Tesla

T1W: T1-Weighted

T2W: T2-Weighted

TBI: Traumatic Brain Injury

Tc-99m-HMPAO: Technetium hexamethylpropyleneamine oxime

TCD: Transcranial Doppler

TCVI: Traumatic Cerebral Vascular Injury

TE: Echo Time

*tid*: three times daily

TORTOISE: Tolerably Obsessive Registration and Tensor Optimization Indolent  
Software Ensemble

TR: Repetition Time

USUHS: The Uniformed Services University of the Health Sciences

UTHSCA: The University of Texas Health Science Center at San Antonio

VCIND: Vascular Cognitive Impairment with No Dementia

VMCI: Vascular Mild Cognitive Impairment

WM: White Matter

WMH: White Matter Hyperintensities

## **CHAPTER 1: INTRODUCTION**

An estimated 1.7 million suffer a traumatic brain injury (TBI) annually in the United States (34), resulting in an economic burden of over \$76.5 billion (36). TBI contributes to about one third of injury related deaths in the United States (34), and is the major cause of disability in children and young adults. Mild TBI (mTBI) is diagnosed in over 85% cases of TBI in the US (32). Most mTBI resolves without long-term symptoms, however, many patients develop symptoms that last years, often resulting in permanent disability. Such post-concussive symptoms include headache, anxiety, dizziness, difficulty sleeping, difficulty concentrating, emotional instability, tinnitus, and memory deficits (101; 108; 133). Unfortunately, there is no gold standard for the diagnosis of mTBI (32). In addition to use of the Glasgow Coma Scale (GCS), other factors are considered, including confusion, disorientation, duration of loss of consciousness, duration of post-traumatic amnesia (PTA), and other transient neurologic abnormalities (20). When these factors support a diagnosis of mTBI, the possibility of intracranial lesion has obligated routine assessment by Computerized Tomography (CT), even though most scans will be normal (32). Often conventional magnetic resonance imaging (MRI) also fails to recognize organic etiology for chronic symptoms (110) suffered by the so-called “miserable minority” (105), underscoring the need to develop reliable clinical biomarkers of injury.

TBI results from both the primary injury, defined as damage resulting from the momentary mechanical insult, and secondary injury, events which evolve in response to the primary injury and contribute more to cell death and functional deficit (19; 69). Therapeutic intervention targets the events of secondary injury, including chemical,

cellular, and metabolic factors, and recent efforts aim to target multiple factors simultaneously (129). It has been emphasized that TBI should be considered a disease process rather than an injurious event. Biochemical and cellular changes may take place days, months, or years after the inciting event. Pro-apoptotic and inflammatory pathways upregulate, often resulting in cell death (80; 85; 115). This is consistent with the emergence of psychiatric deficits days to years after initial injury. Thus, biomarkers of injury would be of clinical value not only to aid in initial diagnosis, but in evaluating the origin of clinical improvements or deterioration over time. Indeed, National Institute of Neurological Disorders and Stroke (NINDS) and Department of Defense consensus meetings have underscored the need to develop imaging and biochemical biomarkers to assess specific pathophysiologic mechanisms relevant to particular pathoanatomic types of TBI, and to test the efficacy of mechanism-specific targeted therapies (28; 61; 106).

At the time of the primary injury, rapid acceleration-deceleration of the head causes differential movement of brain structures due to their variable composition and adherence to the skull or neighboring tissue. Consequently, shearing, tensile, and compressive forces are produced (4). Diffuse injury may include diffuse axonal injury, traumatic subarachnoid hemorrhage, traumatic vascular injury, inflammation, and neuroendocrine dysfunction.

Damage to cerebral blood vessels is well recognized, and inadequate cerebral blood flow (CBF) is believed to contribute significantly to morbidity and mortality (27; 40). Human and animal studies have demonstrated similar pathological evidence of microvascular injury (61) and compelling evidence indicates that enhancing angiogenesis

may improve functional recovery after TBI (21; 77; 121; 122; 136). Non-invasive measures of cerebrovascular function would be of great clinical value, both as a biomarker during evolution of the injury following insult, and in evaluating therapeutic interventions. Magnetic resonance imaging modalities such as Blood Oxygen Level Dependent (BOLD) Imaging, Arterial Spin Labeling (ASL), Transcranial Doppler (TCD), and Near InfraRed Spectroscopy (NIRS) show promising utility, however no method has yet been adopted in routine clinical practice.

The present study establishes a preclinical model to non-invasively measure cerebrovascular function that can be readily adopted in the clinical setting. MRI-ASL was identified as a robust method to assess regional changes in resting CBF longitudinally, and controlled hypercapnia was employed to measure cerebrovascular reactivity: the capacity of the cerebrovasculature to respond to a vasoactive stimulus. This study was designed in parallel to a clinical trial utilizing MRI-BOLD with hypercapnia (ClinicalTrials.gov NCT01797549), which has demonstrated that patients in the chronic stage (>6 months) after moderate to severe TBI exhibit significant reductions in CVR (61).

The success of the pre-clinical model serves as a proof-of-concept for the rapid assessment of novel therapeutic agents. Both studies tested the effect of sildenafil as a cytoprotective treatment, aimed at enhancing angiogenesis. Sildenafil (Viagra; Revatio), a phosphodiesterase type 5 inhibitor, was selected for its favorable safety profile, and effects in animal models of ischemic stroke in increasing CBF, and enhancing angiogenesis, neurogenesis, and axonal remodeling in the penumbra, and in improving functional recovery (30; 76; 143).

Both diffuse axonal injury and microvascular injury have been postulated to contribute to neuropsychological dysfunction after TBI, including in patients with negative radiological findings by conventional CT and MRI (10; 18; 70; 110; 113). Diffuse axonal injury has been well characterized through histology and non-invasively with diffusion tensor imaging (DTI) in these patients, however, the relationship between axonal injury and deficits in cerebrovascular function remains elusive. This study was the first to investigate regional differences in cerebrovascular reactivity (CVR) and changes in microstructural abnormalities.

Given the heterogeneity of primary injury across TBI patients, multiple therapeutic approaches are likely beneficial (28; 56). Incorporating multi-modal neuroimaging in pre-clinical and clinical trials allows investigators to better characterize the interplay between pathophysiologic mechanisms and assess the effect of single or multiple therapeutic interventions.

In summary, this dissertation describes a novel approach to non-invasively assess cerebrovascular function and after TBI. This pre-clinical model can be readily adapted in the clinical setting. Second, this study uses sildenafil as a proof-of-concept for evaluation of pharmacologic or stem cell therapies. The effects of sildenafil on cerebrovascular function and the corresponding histological findings are discussed. Third, this study investigates the relationship between cerebrovascular dysfunction and diffuse axonal injury, the implications of which may guide selection of multiple therapeutic agents in future studies.

## **CHAPTER 2: BACKGROUND**

### **PATHOPHYSIOLOGY OF CEREBRAL MICROVASCULAR INJURY**

Cerebral blood flow has long been postulated to respond to cerebral metabolic demand (104) and its coupling to neuronal activity has been since well described (119). Regional regulation of CBF, as well as its maintenance across a wide range of perfusion pressures, is controlled by the neurovascular unit (NVU) (22; 47). Primary injury results in direct biomechanical disruption of its components, including the vessel wall and the surrounding neurons and glia, causing immediate compromise to the blood-brain barrier (BBB) (100; 111). Events of secondary injury exacerbate breakdown of the BBB, resulting in extravasation of blood and edema, diminished CBF, and focal ischemia (40). CBF deficits have been detected even years after mild TBI, and have been identified as concordant with neuropsychiatric localization (18).

### **PATHOLOGY OF MICROVASCULAR INJURY**

Diffuse vascular injury was first noted as a nearly ubiquitous pathological finding in the brainstem of patients with fatal TBI (125). Scanning electron microscopy of vasculature perfused with mercox in cases of lethal TBI revealed vascular injury evident in both hemispheres, unrelated to the impact zone, and involving predominantly the middle and deep capillary cortical zones. Longitudinal folds, nuclear imprints of endothelial cells, and craters were visualized along the surface of arterioles. Capillaries appeared tortuous, flattened, and often with blind endings (100). Similarly, evidence of microvascular injury in rodent models of TBI has revealed morphological and architectural alterations, including ectasia of pial vessels, sphincter constrictions and



focal swelling of perforating vessels, and widened intercellular junctions, changes resulting in hyperemia, vasogenic and cytotoxic edema, and brain swelling (107).

Traumatic cerebral microvascular injury has also been reported in patients with non-lethal TBI, ranging from mild to severe, who subsequently died of other causes. Perivascular petechial hemorrhages were observed in cases in which macroscopic hemorrhage was not apparent on gross examination (92). Abundant intravascular coagulation in arterioles and venules, particularly in areas of focal contusion, has been identified in human, as well as rat and pig models of TBI, and has been recognized as an important component to secondary injury (116).

### **Chronic Traumatic Encephalopathy**

Athletes in the National Football League with a history of concussion and cognitive or psychiatric impairment have demonstrated a constellation of neuropathologic findings on autopsy, including the presence of multifocal or diffuse tau-positive neurofibrillary tangles (NFTs) and neuritic threads, and an absence of neuritic amyloid plaques, other tauopathies, and Lewy bodies. These features have been used to identify the progressive neurodegenerative syndrome following blunt force trauma or acceleration-deceleration injuries to the brain, referred to as chronic traumatic encephalopathy (CTE) (91). While classically studied in professional athletes, CTE may occur in players of elementary, high school, or collegiate level contact sports, in military personnel exposed to blast and other indirect or direct injury, and in victims of physical abuse (39; 117). Recent consensus panels funded by the National Institute of Neurological Disorders and Stroke (NINDS) and National Institute of Biomedical

Imaging and Bioengineering (NIBIB) have defined the pathognomonic neuropathological feature for diagnosis of CTE as the presence of hyperphosphorylated tau in neurons and astroglia accumulated in an irregular pattern around small blood vessels at cortical sulci (87). Hemosiderin also has been noted to accumulate in perivascular macrophages, neuroglia, and the extracellular space, particularly at the meninges, subpia, and cerebellar folia (1). Animal studies have identified similar neuropathologic features of CTE. In a mouse model of blast-induced TBI, hippocampal capillaries exhibit thickened tortuous basal lamina, abnormal endothelial cells with irregularly shaped nuclei, surrounded by edematous and vacuolated astrocytic foot processes (42). Further studies are indicated to validate the diagnostic criteria for CTE and to understand the contribution of microvascular injury to the development of disease.

#### **IMAGING TRAUMATIC CEREBRAL VASCULAR INJURY: CLINICAL STUDIES**

Non-invasive imaging techniques have revealed increasing evidence for traumatic cerebral vascular injury (TCVI) in cases of mTBI. Susceptibility weighted imaging (SWI) detects differences in the phase and magnitude of signals generated from tissues with heterogeneous magnetic susceptibilities due to, for example, differences in the amount of calcium, or iron in the form of deoxyhemoglobin, ferritin, or hemosiderin. SWI has been used to study several pathologic states, including multiple sclerosis, stroke, vascular malformations, tumors, aging, and trauma (46). It is particularly sensitive to detecting microhemorrhages during the acute period after injury, and detecting hypoxic ischemic secondary injury (55). SWI has been shown to have superior detection of hemorrhagic diffuse axonal injury than conventional gradient echo (GRE) imaging, both in the number

and volume of hemorrhagic lesions (127). In a follow up study of children and adolescents with mild to severe TBI, these two factors were found to negatively correlate with neurological outcome (126). Microhemorrhages have been identified in about a quarter of patients with mTBI in the subacute period. Presence of microhemorrhages was also associated with short term memory deficits in these patients, indicating SWI's utility as a severity biomarker across the full spectrum of TBI (54).

Several neuroimaging methods have been developed over the last few decades that have shed light on the functional deficits related to TCVI. Deficits in cerebral blood flow have been reported in clinically symptomatic patients even years after mild TBI. Technetium hexamethylpropyleneamine oxime (Tc-99m-HMPAO) single photon emission computed tomography (SPECT) imaging revealed regions of hypoperfusion in frontal, prefrontal, and lateral cortices in such patients, despite lack of structural abnormality on CT or MRI (18). Increased brain activity drives an increase in blood flow, detected by SPECT imaging as an increase in uptake of radiolabeled tracer, allowing determination of regional brain metabolism (55). However, it is difficult to distinguish whether deficits in brain metabolism are due to vascular or neuronal injury. In animal studies, cranial windows allow direct visualization of cortical vessels after TBI, and have revealed impaired CVR to vasodilators, including acetylcholine, carbon dioxide, and to the nitric oxide donor sodium nitroprusside (132).

Measuring CVR allows more direct assessment of vascular health. In clinical settings, TCD, SPECT, and positron emission tomography (PET) have been implemented to assess CVR. TCD measures blood flow velocity in the middle cerebral artery (MCA<sub>v</sub>). Professional boxers with chronic TBI, as well as athletes with recent mild TBI, exhibit

impaired CVR between hyper- and hypocapnia challenges, as indicated by attenuated changes in  $MCA_v$  (6; 73). Additionally, boxers demonstrated decreased cortical oxygenation during orthostatic challenge compared to controls, as assessed by continuous near infrared spectroscopy (NIRS) (6). While TCD and NIRS offer low cost and rapid assessment of CVR, low spatial resolution and an inability to measure regional differences precludes whole-brain mapping. Both SPECT and PET are expensive and require exposure to radiation, limiting their clinical utility (43; 74). MRI methods allow whole-brain mapping of CVR and do not require exposure to radiation.

MRI under carbon dioxide ( $CO_2$ ) inhalation affords quantitative and non-invasive assessment of CVR. Two such methods include Blood Oxygen Level Dependent (BOLD) imaging and Arterial Spin Labeling (ASL). The BOLD signal is generated by changes in the magnetic susceptibility of the tissue caused by changes in the amount of paramagnetic deoxyhemoglobin (dHb) in venous blood, which attenuates the MR signal (90). An increase in blood  $CO_2$  partial pressure causes vasodilation, resulting in an increase in blood flow and blood volume (45) without changing the metabolic rate of oxygen consumption ( $CMRO_2$ ) (62). Consequently, the paramagnetic dHb becomes diluted, resulting in less attenuation of the magnetic resonance (MR) signal (52). Thus, the BOLD signal measures CVR indirectly (60).

ASL measures CBF and is therefore a more direct measure of CVR (43). ASL has been used extensively to study CBF in rodent models of TBI (37; 50; 51; 65), generally using a field strength of 4.7 Tesla (T). However, signal averaging is time-consuming (26) and its signal-to-noise ratio is poor at 1.5 T, the standard field strength in clinical settings, which has precluded its widespread clinical use (43). Nevertheless, improvements in ASL

methodologies has led to its utilization in evaluating perfusion abnormalities in patients with migraine (97), seizure (98), stroke (15; 84), and TBI (64; 128). For example, ASL has revealed impaired regional cerebrovascular reactivity (CVR) to acetazolamide in patients with carotid artery stenosis or occlusion (16; 17).

Given its sensitivity in detecting differences in the magnitude of CBF changes in response to hypercapnia, ASL was selected as the optimal imaging modality to evaluate CVR. The clinical trial that this study parallels has utilized hypercapnia BOLD, with preliminary results showing that patients with moderate to severe TBI tend to have more variability and overall lower CVR values (61). Long et al. (81) recently assessed the regional and temporal CBF response to hypercapnia in rodents subjected to controlled cortical impact (CCI). Interestingly, regional alterations in CBF and the cerebrovascular response to hypercapnia were greater than alterations in T2 relaxation time, apparent diffusion coefficient (ADC), and fractional anisotropy (FA) (81), highlighting the superior sensitivity of CVR assessment methods. The present study expands upon this work in utilizing an injury model that produces diffuse cerebrovascular injury, and more closely mimics human injury compared to CCI. This model, termed fluid percussion injury, is discussed further below.

#### **CANDIDATE PRO-ANGIOGENIC TREATMENTS**

To date, most clinical trials of therapeutic interventions for TBI have focused on neuroprotection (135); few have attempted to improve function by restoring vascular health (clinicaltrials.gov identifiers NCT01762475, NCT00313716). In rodent models of TBI, L-Arginine improved CVR (41), Arginase II-knock outs showed superior restoration

of CBF (14), and inhaled nitric oxide (NO) therapy improved CBF, reduced lesion volume, and improved neurological recovery (121). We have selected Sildenafil (Viagra; Revatio), a phosphodiesterase type 5 inhibitor, to enable the endogenous response of NO production to function more effectively. In animal models of ischemic stroke, sildenafil has been shown to be effective in increasing local cerebral blood flow, and enhancing angiogenesis, neurogenesis, and axonal remodeling in the penumbra, and in improving functional recovery (30; 76; 143). The dose and timing of sildenafil we implemented is based on the success of sildenafil in these studies. Sildenafil has also improved deficits in cerebrovascular reactivity in patients with pulmonary hypertension, without affecting overall CBF (103).

We have selected sildenafil for its capacity to potentiate NO signaling and its favorable safety profile. Certainly, several other FDA-approved pharmacologic agents exist that target the same pathway. For example, sodium nitroprusside (SNP) spontaneously releases NO to dilate both arteries and veins. Although SNP has been shown to effectively increase vessel diameter, it is very short-acting and its side effects, including hypotension, cerebral edema, nausea, vomiting, migraine, and cyanide poisoning, preclude its clinical use. Similarly, nitroglycerin may cause systemic hypotension and rebound hypertension upon cessation of drug delivery (33). Nevertheless, in rodent models of TBI, the NO donor (Z)-1-[2-(2-aminoethyl)-N-(2-ammonioethyl)amino]diazene-1,1,2-diolate (DETA/NO<sub>2</sub>Oate) increased neurogenesis and improved function (83), S-nitroso-N-acetylpenicillamine (SNAP) reversed impaired CVR to hypercapnia (142), and the nitrosylating agent S-nitrosoglutathione reduced secondary injury in rodent models of TBI (63), suggesting that new generation NO

donors also hold potential as therapeutic agents. Pre-clinical models of TBI have also shown promising results for the use of FDA-approved statins and sulfonylureas in promoting angiogenesis and attenuating secondary injury (71; 131).

## **DIFFUSE AXONAL INJURY**

### **White Matter Damage and Vascular Dysfunction**

Although the interplay between cerebrovascular dysfunction and white matter damage in the development of neurologic dysfunction has not been widely studied in the field of TBI, such mechanisms have been postulated in dementia, stroke, and the aging population (57; 102; 120). White matter hyperintensities (WMH) on conventional MRI have been associated with cerebrovascular risk factors including diabetes (89; 140), cardiac disease (59; 140), and hypertension (31; 82; 93). This is not surprising, as white matter is known to be particularly vulnerable to ischemia (93). Iadecola provides an excellent review of several conditions in which vascular factors may alter white matter integrity and lead to cognitive impairment, including hypoperfusion dementia, leukoariosis, microhemorrhages, Cerebral Autosomal Dominant Arteriopathy with Subcortical Infarcts and Leukoencephalopathy (CADASIL), and cerebral amyloid angiopathy (57).

In a transcranial Doppler study, Novak et al. showed that diabetic patients exhibited decreased blood flow velocity (BFV) in the middle cerebral arteries, impaired reactivity to hypo- and hypercapnia, and that WMH correlated negatively with baseline BFV (89). Impaired cerebrovascular reactivity has also been shown to correlate with the presence of asymptomatic WMH (58) and WMH in elderly (7). Given the widespread

cerebrovascular injury in TBI discussed in the above sections, it is plausible that cerebrovascular dysfunction may similarly correlate with, or contribute to, white matter damage and neuropsychological sequelae.

### **Effect of Vascular Injury and White Matter Lesions on Cognitive Function**

Pathologic studies of elderly, depressed patients have reported increased vascular lesions in the white matter (123). These ischemic lesions were in support of the notion of “Vascular Depression” proposed by Alexopoulos in 1997 (2), linking cerebrovascular disease to the development of geriatric depressive syndromes. Since then, various studies have explored the hypothesis that underlying vascular mechanisms may give rise to development of depression in the elderly. Other evidence for the development of depressive symptoms points to WM changes as assessed by DTI (120). In a study of 22 patients with vascular cognitive impairment with no dementia (VCIND) who were compared to 28 normal controls, evidence of microstructural white matter damage (see table 1) was found in all projection fibers, association fibers, and commissural fibers. Furthermore, cognitive function as assessed by the Montreal Cognitive Assessment correlated positively with fractional anisotropy (FA) values and negatively with mean diffusivity (MD) values (79). Similarly, a multicentric study of patients with vascular mild cognitive impairment (VMCI) revealed an association between depressive symptoms and WM microstructural damage as measured by DTI scalars. Of note, this study did not observe an association between depressive symptoms and WMH, which may have been due to, at least in part, DTI’s superior sensitivity to early WM damage



compared to evaluation of WMH by conventional fluid-attenuated inversion recovery (FLAIR) imaging (95).

### **White Matter Damage in TBI**

Compared to conventional CT and MRI scans, DTI has shown superb capability at identifying diffuse axonal injury (DAI). This highlights its potential use as a biomarker for initial injury diagnosis and for the characterization of white matter changes over time. In general, damage to white matter integrity is expected to result in decreased fractional anisotropy (FA) and increased mean diffusivity (MD). However, reports of increased FA and decreased MD following injury have led authors to suspect that such changes may be indicators of poor prognosis. Shenton et al. (2012) provides an excellent summary of DTI findings, several of which are also listed in Table 1 (110). One hypothesis for increased FA and decreased MD is that the restricted diffusion of water is result of cytotoxic edema and axonal swelling, whereas the opposite findings may reflect the vasogenic edema which is more likely to resolve over time (11; 66). Injury severity has also shown variability in DTI findings, suggesting different pathological mechanisms. In a study which included mild, moderate, and severe TBI, both axial diffusivity (AD) and radial diffusivity (RD) were increased in WM regions in the moderate to severe cases, whereas the mild cases showed only increases in AD, suggesting that axonal damage, but not myelin damage, was present significantly in these patients (67). Others have found reduced RD concomitant with increased FA in mTBI patients (86), which may be explained by cytotoxic edema, nevertheless highlighting the heterogenous nature of TBI.

Considerable variability in DTI findings may also relate to the length of time post-injury, magnetic strength, brain regions examined, and analytic methods (110).

Preclinical studies have revealed similar persistent microstructural changes. For example, *in vivo* DTI of rats 6 months after severe TBI by fluid percussion injury demonstrated decreased FA and increased RD in the splenium of the corpus callosum and internal capsule, and increased MD in the splenium of the corpus callosum, ipsilateral to the lesioned hemisphere (72).

Given the established relationship between microvascular disease and white matter damage in other disease states, and their association with neurocognitive deficits, there is high likelihood that vascular damage after TBI may also result in disruption in WM integrity, providing a plausible mechanism to account for neurocognitive sequelae of TBI. If correlation is identified between vascular and axonal injury, further work would be indicated to identify the temporal relationship. If vascular injury precedes axonal injury, this provides meaningful information for the timing of administration of mechanism-specific therapeutic interventions.

Table 1. DTI findings in vascular disease and after TBI. Changes in DTI parameters show similar patterns. Refer to text for exceptions, italicized below.

Study Subjects	DTI Parameters	Correlation	Reference
Vascular Cognitive Impairment with no Dementia (VCIND)	Decreased FA (WM) Increased MD (WM)	Worse cognitive function	Lin et al. (2015) (79)
Vascular Mild Cognitive Impairment (VMCI)	Decreased FA (WM) Increased MD (WM)	More depressive symptoms	Pasi et al. (2015) (95)
24hr post-mTBI	Decreased FA (WM) No change in MD	-	Arfanakis et al. (2002) (5)
4d & 6mo post-mTBI	Decreased FA (WM) Increased MD (WM)	Cognitive measures correlated at 6mo, not at 4d	Miles et al. (2008) (88)
3d post-mTBI	<i>Increased</i> FA - May indicate axonal swelling	Post-concussive score	Bazarian et al. (2007) (11)
Mild-mod TBI: symptomatic vs asymptomatic	<i>Increased</i> FA <i>Decreased</i> ADC (mesencephalon)	Presence of symptoms	Hartikainen et al. (2010) (48)
Mild, mod, severe TBI	Decreased FA; Mod-severe: AD & RD incr (WM) Mild: Incr AD, no change MD	-	Kraus (2007) (67)
21d post-mTBI	<i>Increased</i> FA and Decreased RD (WM)	-	Mayer et al. (2010) (86)

## **ANIMAL MODEL**

### **Animal Selection**

Experiments were performed using male Sprague-Dawley (SD) rats weighing 250-350 grams. The SD rat was the first strain utilized when the fluid percussion injury (FPI) model was initially adapted to the rat. Since then, SD rats have been widely used to study hemodynamic changes following FPI (29; 137; 141) and to characterize the cerebrovascular response to hypercapnia (8; 9; 112; 132). Since estrogen is known to enhance NO production by increasing endothelial nitric oxide synthase expression and activation (3), and CVR has been demonstrated to vary across the menstrual cycle in humans (68), female rats were not included to reduce potential confounding variables related to dynamic hormone levels. Additionally, female rats demonstrate a much slower plasma clearance of sildenafil and longer elimination half-life compared to male rats, consistent with gender differences in cytochrome P450 metabolism in this species (130). Young adult rats were chosen for study given the predominance of military and civilian personnel affected by TBI in this age group (24).

### **Fluid Percussion Injury**

The FPI model produces both focal and diffuse damage, and mimics histopathological features of human closed head injury (124). Microvascular damage is apparent in the region of the contusion and perilesional sites (78; 94) and over three decades of research describe the hemodynamic changes (12; 29; 75; 141). FPI results in acute regional CBF (rCBF) depression in cortical and subcortical regions (29; 137; 141), and altered rCBF 8 months after injury (49). Furthermore, FPI results in diminished CVR

to hypercapnia, acetylcholine, adenosine, and nitric oxide donors (132). Thus, FPI produces reproducible injury characteristics similar to those observed in human, providing the ideal paradigm for developing a method to non-invasively assess CVR and response to therapy.

### **Defining Sham**

For behavioral testing and histological analyses, the sham group received the same duration of anesthesia as the injured groups, a scalp incision, and skull clearing. Tissue edema and bleeding associated with incision and skull clearing produce regional susceptibility differences detected by MRI. Such differences are capable of producing artifacts on echo planar imaging, particularly along the cortical surface, making control for this variable crucial in the sham group. Moreover, craniotomy has been associated with microvascular damage and arteriolar vasoconstriction secondary to loss of tissue CO<sub>2</sub>, and was therefore not performed in sham animals, consistent with recent recommendations to utilize anesthesia-only controls to avoid injury associated with craniotomy procedures (23).

## CHAPTER 3: SPECIFIC AIMS

Traumatic brain injury (TBI) contributes to about one third of injury related deaths in the United States, (35) and is the major cause of disability in children and young adults. Damage to cerebral blood vessels is well recognized after TBI, and inadequate cerebral blood flow (CBF) is believed to contribute to morbidity and mortality (27; 40). Diffuse axonal injury, which often coexists with diffuse vascular injury, has also been postulated to contribute to neuropsychological dysfunction (110), however the relationship between the two endophenotypes in the pathogenesis of disease remains unknown. *We hypothesize that traumatic cerebral microvascular injury after TBI can be measured non-invasively, correlates with axonal injury, and is amenable to therapeutic intervention.*

Angiogenesis after injury may occur by division of mature endothelial cells of the parent vasculature or by integration of bone marrow derived endothelial precursor cells into newly formed blood vessels at the site of injury (135). Enhancing this process may restore local perfusion, promote neuronal survival, and improve functional recovery. We hypothesize that potentiating nitric oxide signaling through administration of the phosphodiesterase 5 inhibitor, sildenafil, will facilitate vascular recovery.

**AIM 1: *Validate a method to non-invasively assess the extent of cerebrovascular deficits in young adult male rats following moderate traumatic brain injury.*** A focal and diffuse, non-penetrating injury will be administered by a well-established rodent model of TBI, fluid percussion injury (FPI). Magnetic resonance imaging (MRI) under CO<sub>2</sub> inhalation affords quantitative and non-invasive assessment of

cerebrovascular reactivity (CVR), a measure of vascular function. CVR will be assessed using Arterial Spin Labeling (ASL). Deficits in CVR will be compared to neurobehavioral outcome and histopathologic measures. Neurobehavioral measures will include the Neurologic Severity Score, Morris water maze, Rotarod, and Open Field Test. The results of the non-invasive imaging will be compared to histological assessments, including immunohistochemistry with antibodies to RECA-1 (microvessels), GFAP (astrocytes), and Iba-1 (microglia). We hypothesize that rats exposed to FPI will demonstrate deficits in CVR, which will correlate with neurobehavioral deficits and histopathological findings.

***AIM 2: Test the effect of sildenafil as a cytoprotective treatment.***

Cerebrovascular reactivity (CVR), neurobehavioral outcome, and histopathology following sildenafil treatment will be evaluated. Methods outlined in Aim 1 will be utilized. Subcutaneous sildenafil will be administered daily for 7 days, beginning 1 hr post-injury. We hypothesize that sildenafil will attenuate CVR deficits, and improve neurobehavioral and histological outcome.

***AIM 3: Investigate the relation of cerebrovascular injury with axonal injury.***

MRI will be used to assess microstructural changes after injury reflective of diffuse axonal injury (DAI) using diffusion tensor imaging. We hypothesize that DAI, as indicated by decreased FA values and increased MD values in white matter, will be observed after FPI, and that regional changes will correlate with compromised CVR.

## CHAPTER 4: METHODOLOGIES

### STUDY PARADIGM

All housing, surgical, and perioperative procedures were performed in accordance with the Uniformed Services University of the Health Sciences Institutional Animal Care and Use Committee, and the Center for Neuroscience and Regenerative Medicine Standard Operating Procedure for Brain Injury Models. Male Sprague-Dawley (SD) rats weighing 250-350 grams were obtained from Charles River. The study time line is depicted in Figure 1, below.

All aspects of husbandry and care were performed in accordance with LAM Husbandry standard operating procedures and the Guide for Care and Use of Laboratory Animals. Animals were housed two animals per cage. Food and water were provided *ad libitum*. A 12-hr reverse light cycle was maintained. Animals were acclimated for at least 7 days to the vivarium and the reverse light cycle conditions before they were used for any study. The animals were observed daily for general health, humane treatment, and husbandry considerations.

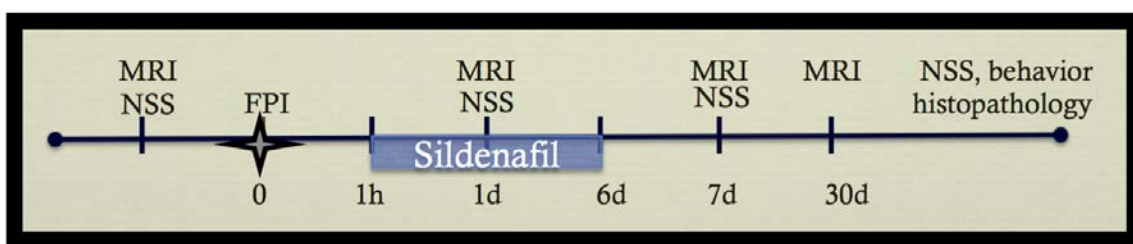


Figure 1. Study Paradigm.

Baseline MRI and NSS were performed the week preceding surgery. Rats received either FPI or sham-FPI followed by either saline or sildenafil treatment. NSS was assessed at 24 hours after surgery, and repeated on days 3, 5, 7, 14, 21, and 28. MRI was acquired 1d, 7d, and ~30d after surgery. Additional behavioral tests were performed one month after surgery.



## **SURGICAL PROCEDURES**

Rats were anesthetized in an induction chamber with a mixture of isoflurane in oxygen (3-4%). The rodent's head was shaved, and the animal placed on a rat bed with a circulating warm-water circuit to maintain body temperature, and the head fixed in a stereotaxic device equipped with nose cone. Anesthesia was maintained with <2% isoflurane. The skin was cleaned with Betadine and alcohol prep pads and the skull exposed using a small surgical incision over the midline scalp. The skull was cleared of connective tissue, minimizing disruption of the temporalis muscles. A circular craniotomy 5mm in diameter was made midway between bregma and lambda, with the medial edge 1 mm to the right of the sagittal suture, leaving the dura intact. A female luer coupler was fixed to the skull with cyanoacrylic glue and dental cement, through which a moderate impact pressure (4.5 atm) was delivered. The peak pressure pulse delivered was recorded. The sham group received the same duration of anesthesia and only the incision and skull clearing were performed. Saline or sildenafil (10mg/kg) was injected subcutaneously beginning 1 hour after impact, and daily for a total of 7 days.

## **MRI METHODS**

Images were acquired on the Bruker BioSpec system (Bruker NMR, Inc., Billerica, MA) that consists of a 7-Tesla (T), 20-cm horizontal bore, and superconducting magnet (Magnex Scientific, Abingdon UK), and is equipped with an 86mm quadrature transmit coil, and a dedicated phased array head coil. The neck coil was developed at the National Institutes of Health (NIH) for perfusion labeling (114).

Animals were anesthetized in an induction chamber with a mixture of isoflurane in oxygen (3%) and maintained with a mixture of isoflurane in medical air delivered by nose cone (1-2% isoflurane in 30% O<sub>2</sub> and 70% N<sub>2</sub>, 3 liters per minute (LPM)). CO<sub>2</sub> was continuously monitored and recorded by capnograph (Smiths Medical, Dublin, OH) by placing the sampling tube in the nose cone. The animals were placed in a rat bed with a circulating warm-water circuit to maintain body temperature. Respiratory rate, heart rate, saturation of peripheral oxygen (SpO<sub>2</sub>) and rectal temperature was monitored continuously (SA-instruments, Stony Brook, NY; Harvard Apparatus, Holliston, MA). Anesthesia was adjusted as necessary to maintain respiration near 55 breaths per minute.

The total duration of the imaging protocol at all time points was limited to approximately 60 minutes. There were approximately 15 minutes for animal preparation, positioning, and MRI shimming before the serial MRI scans. All animals received the following set of MRI scans: the anatomical proton density/T2 weighted (PDW/T2W) imaging and T1 weighted (T1W) structural imaging for injury assessment, structural changes, and edema formation; Susceptibility Weighted Imaging (SWI) for detection of traumatic hemorrhagic lesions; ASL to calculate cerebral blood flow at rest and during hypercapnia; and the BOLD time-series to assess dynamic cerebrovascular reactivity to hypercapnia.

The MRI procedures to assess cerebrovascular responses were adapted from Yezhuvath et al. (139), and Sicard et al. (112), as follows. Hypercapnia was induced by changing the inhaled gas composition to 5% CO<sub>2</sub> in medical air using a 3-way valve. Anatomic images (PDW, T2W, and T1W), the T1 map, and labeling efficiency (collective 20 min), SWI (4 min), DTI (8 min), and baseline ASL (6 min) were acquired

with animals breathing medical air (MA). The hypercapnia trial included 11 min BOLD, which began with 60 sec MA followed by alternating 60 sec hypercapnia and MA, then ASL during hypercapnia (6 min). The present study focuses on ASL and DTI; analysis of other modalities will be performed in future studies.

### **Arterial Spin Labeling (ASL)**

Continuous arterial spin labeling (CASL) was used to non-invasively quantify cerebrovascular reactivity (CVR) by assessing CBF (114). CBF measurements were made using a four-shot EPI with repetition time (TR)=7s, time to echo (TE)=20ms, multiple repetitions (n=6, 6 minutes) of the interleaved control and labeling acquisitions, and a full brain coverage using the dedicated perfusion labeling neck coil. All images were acquired with 200um<sup>2</sup> in-plane resolution, slice thickness 800um. Resting CBF was assessed with the animal breathing medical air (MA, 30% O<sub>2</sub> and 70% N<sub>2</sub>, 3 LPM) over 6 minutes. Hypercapnia was induced by changing the inhaled gas composition to 5% CO<sub>2</sub> in medical air (30% O<sub>2</sub>, 65% N<sub>2</sub>, 5% CO<sub>2</sub>, 3 LPM) using a control valve. The imaging sequence to measure CBF during hypercapnia was initiated 60 sec after turning the valve, and images were acquired for the following 6 min. CVR was measured as the regional percent change in CBF:  $CVR = \frac{CO_2-MA}{MA}$ .

### **Diffusion Tensor Imaging**

DTI data were acquired using a two-dimensional (2D) spin echo sequence with TR=3.75s, TE=24msec, field of view (FOV)=25.6x25.6mm, spatial resolution=0.160 mm/pixel, slice thickness=1mm. Diffusion weighting was applied to 12 uniformly distributed directions (Gradient Separation (Δ)=12msec, diffusion gradient duration

( $\delta$ )=3.5 msec, three  $B_0$ 's,  $b$ -value=1000 s/mm<sup>2</sup>). Two averages were acquired. The total scan duration for DTI data was 8 min.

### **Data Analysis**

After acquisitions, imaging data was downloaded from Bruker Paravision 5.1 (Bruker Biospin, Inc., Billerica, MA) and transferred. For ASL processing, 2dseq images were converted to NIfTI images with MIPAV software (NIH, Bethesda, MD). CBF maps were created using FSL (Analysis Group, FMRIB, Oxford, UK) and analyzed with VivoQuant (InviCRO, Boston, MA) using region of interest (ROI) and atlas based approaches. DTI data were analyzed using TORTOISE (NICHD, Bethesda, MD) (96) and Mango software (UTHSCA, San Antonio, TX).

Statistical analysis was performed using Prism 6.0 (GraphPad Software, Inc.). Two-way repeated measure ANOVA was utilized with time as the repeated measure. Multiple comparisons were performed for each ROI by comparing the mean value post injury to the mean value at baseline. Correction for multiple comparisons was performed with Sidak's test. For correlation analyses, the Spearman  $r$  was calculated using a 95% confidence interval. Two tailed  $p$ -values were calculated with significance defined as an alpha value of 0.05. False discovery rate (FDR) correction for multiple comparisons was performed with Microsoft Excel, using a FDR set to 0.05.

### **NEUROBEHAVIORAL TESTING**

Animals were transported from the housing room to the behavioral testing room, and testing was performed in the day time on all animals (maintained on reverse light cycle). Neurobehavioral deficits were assessed using the Neurological Severity Score

(NSS, see appendix). The NSS was performed at baseline and post-injury days 1, 3, 5, 7, 14, 21, and 28. The revised NSS (NSS-R) was also utilized to assess possible enhanced sensitivity to neurologic deficits (134; 138). The NSS-R was incorporated after the study had been initiated, and was therefore performed on a subset of animals. The NSS-R was performed after the NSS, so as to avoid potential confounding factors on the NSS. Where applicable, neuroscores were assessed prior to MRI to minimize confounding effects of stress and anesthesia. Late neurobehavioral deficits were assessed during the week of the final scan (28-31 days post injury), using the Morris Water Maze, Rotarod, and Open Field testing.

### **Rotarod**

The Rotarod (San Diego Instruments, Inc., San Diego, CA) was used to assess motor coordination. Rotarod testing consisted of two training days and one test day. On day 1, rats were placed on a rotating rod at constant speed (10 rotations per minute (RPM)) until able to remain on the rod for 90 sec without falling. Day 2 consisted of 4 trials with 2-minute inter-trial intervals: trial 1 was the same as day 1 (90 sec at 10 rpm), trials 2 and 3 were 200 sec at increasing speed (0-20 rpm), and trial 4 was 240 sec at increasing speed (0-30 rpm). The test day consisted of 3 trials, each for 240 sec at increasing speed (0-30 rpm). On test day, the latency to fall from the rod was measured for each trial and averaged for a final score.

## **Morris Water Maze**

The Morris Water Maze was used to assess hippocampal-dependent learning and memory. The maze consisted of a water tight pool 135 cm in diameter and 60 cm deep. The pool was equipped with a built in heater and thermostat to control the water temperature at 22 - 24°C. The pool was filled with water to a depth of 50 cm. A circular platform 12.5 cm in diameter was placed 1.5 cm below the surface of the water. The water was made opaque by mixing 250 ml of white non-toxic paint (*Washable Poster Paint* from Palmer Paint Products Inc. (Troy, MI) or *Fresco Tempera Paint* from Rich Art Color Company (Northvale, NJ)) into the water. Four salient shapes were taped to the North, South, East, and West side of the pool, with the lowest edge of the shapes about 5 cm above the surface of the water. Visual markers in the testing room included a wall, laboratory bench, and shelving. Other potentially salient visual markers, such as area lighting or computer screens, were absent from the testing room.

Each test day consisted of 5 trials. Briefly, rats were allowed to swim 120 sec to find a hidden platform. Examiners existed the room immediately upon initiation of each trial. If the rat failed to find the platform, the examiner entered the room and guided the rat to the platform. The rat was allowed to remain on the platform for 30 sec. The rat was then gently towel-dried and allowed to rest in a home cage for 60 sec between trials. The first 3 days of testing, the platform remained in the same position. On the 4<sup>th</sup> day of testing, the platform was placed in a new position. Time to platform and, on the 4<sup>th</sup> day, time spent in correct quadrant was recorded by the Any-Maze tracking system and analyzed by investigators blind to experimental group.

## **Open Field Testing**

The Open Field Test was performed on day 4 of behavioral tests, prior to the Rotarod test. Rats were placed in a circular arena with bedding (74 cm diameter x 16.5 wall height) and allowed to explore for 5 min. An overhead camera recorded the path traveled and events were reported by the Any-Maze tracking system. Total distance travelled was used to assess locomotive function. Time spent moving versus freezing and total time spent in the central versus peripheral regions of the arena was used to assess anxiety-like behavior.

## **HISTOLOGY**

Animals were anesthetized by intraperitoneal (*ip*) administration of ketamine (50-100 mg/Kg) and xylazine (5-10 mg/Kg) and perfused transcardially with saline then 4% paraformaldehyde (PFA) in 0.1M phosphate buffered saline (PBS) (pH 7.4). Brains were removed and soaked in 4% PFA overnight, then fixed in 20% sucrose in 0.1 M phosphate buffer overnight, and placed in fresh 20% sucrose until brains sunk in solution. Brains were frozen and stored at -80 C. 20 to 30-um sections were cut by cryostat in the coronal plane and immunostained by FD Neurotechnologies (Columbia, MD) according to the following provided methods. Blood vessels were identified by RECA-1 (Abcam, Cambridge, MA), astrocytes with GFAP (BD Biosciences, San Jose, CA), and microglia with Iba-1 (Wako Chemicals, Richmond, VA).

Thirty  $\mu$ m free-floating sections of rat brains (3 sections per brain, approximately through the regions from Bregma -3.96mm to -5.80mm) were processed for  $\beta$ -APP-

immunostaining according to the method described by Stone et al. (118) for future study. Briefly, after washes in 0.01 M PBS, pH 7.4) and inactivating the endogenous peroxidase activity with hydrogen peroxidase, sections were placed in 0.1 M citric buffer (pH 6.0) and microwaved at 45°C for 5 minutes. Following 20 minutes of cooling at room temperature, sections were pre-incubated for 40 min in PBS containing 10% normal goat serum (NGS) (Vector Lab., Burlingame, CA) and 0.3% Triton X-100 (Sigma, St. Louis, MO). Sections were then incubated for 40 hours at 4°C in PBS containing 1% NGS and the rabbit antibody to the C-terminus of the human beta-APP (1:2,000) (Invitrogen, Carlsbad, CA, Cat. #51-2700). Subsequently, the immunoreaction product was visualized according to the avidin-biotin complex (ABC) method of Hsu et al. (53) with the Vectastain elite ABC kit (Vector Lab.). Sections were incubated in PBS containing a biotinylated goat anti-rabbit IgG, Triton-X and NGS for 1 hour and then in PBS containing an avidin-biotinylated horseradish peroxidase complex for another hour. This was followed by incubation of the sections for 5 minutes in 0.05 M Tris buffer (pH 7.2) containing 0.03% 3',3'-diaminobenzidine (Sigma) and 0.0075% H<sub>2</sub>O<sub>2</sub>. All steps were carried out at room temperature except where indicated, and each step was followed by washes in PBS. After thorough rinses in distilled water, sections were mounted on gelatin-coated microscope slides, dehydrated in ethanol, cleared in xylene, and coverslipped in Permount® (Fisher Scientific, Fair Lawn, NJ).

For GFAP (BD Biosciences, San Jose, CA, Cat. No. 5556330), Iba-1 (Wako Chemicals, Richmond, VA, Cat. #019-19741), and RECA-1 (Abcam, Cambridge, MA, Cat. No. ab9774) staining, after inactivating the endogenous peroxidase activity with hydrogen peroxidase, sections were incubated separately with avidin and biotin solutions



(Vector Lab, Burlingame, CA) for blocking nonspecific binding of endogenous biotin, biotin-binding protein and lectins. Sections were then incubated free-floating in 0.01 M PBS (pH 7.2) containing the normal blocking serum, Triton X-100 and the specific antibody for 65 hours at 4°C using dilution factors of 1:2,500 for GFAP, 1:15,000 for Iba-1, and 1:1,000 for RECA-1. Subsequently, the immunoreaction product was visualized according to the ABC method of Hsu et al. with the Vectastin elite ABC kit (Vector Lab., Burlingame, CA) and 3',3'-diaminobenzidine (Sigma, St. Louis, MO) as a chromogen. After thorough washes, all sections were mounted on microscope slides. Following dehydration in ethanol, sections were cleared in xylene, and coverslipped in Permount® (Fisher Scientific, Fair Lawn, NJ).

All slides were scanned using a NanoZoomer (Hamamatsu, Bridgewater, N.J.). Digitized files were converted using the NDPITools plugin (25) and analyzed with FIJI (109).

## **CHAPTER 5: RESULTS**

### **ANIMALS EXCLUDED FROM STUDY**

Out of the 15 animals used for the present study, one animal was excluded due to excessive bleeding and possible puncture of dura mater during the FPI surgery. Any animal found to have a missing limb or hydrocephalus during baseline scans was replaced by the vendor and was not included in the study.

### **AIMS 1 & 2: A NON-INVASIVE MODEL TO ASSESS CEREBROVASCULAR DEFICITS AND RESPONSE TO THERAPEUTIC INTERVENTION**

#### **Arterial Spin Labeling Detects Deficits in Cerebrovascular Function after TBI**

At baseline, prior to FPI or sham surgery, cerebrovascular function was assessed non-invasively by measuring CBF using arterial spin labeling. Mean CBF values for the ROIs shown in Figure 2 were 65-75 mL/min/100g during MA and 83-96 mL/min/100g during hypercapnia. Following FPI, 2-way ANOVA of resting CBF revealed a significant main effect for both time ( $p=0.0028$ ) and subjects ( $<0.0001$ ). Bonferroni's multiple comparisons analysis showed a significant reduction in CBF during MA for the right auditory cortex at days 7 and 30 post injury compared to baseline (Figure 3), and during hypercapnia at day 30 post injury compared to baseline (Figure 4) in saline treated animals.

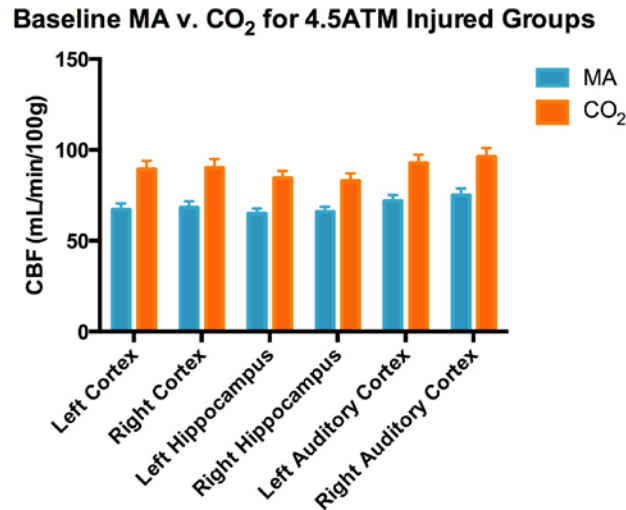


Figure 2. Effect of Hypercapnia on CBF.

Hypercapnia (5% CO<sub>2</sub>) resulted in a statistically significant increase in CBF compared to medical air (MA) across all ROIs in rodents. Measurements were performed at baseline, the week before fluid percussion injury (main effect of air type  $p < 0.0001$ , error bars represent SEM,  $n = 15$ ).

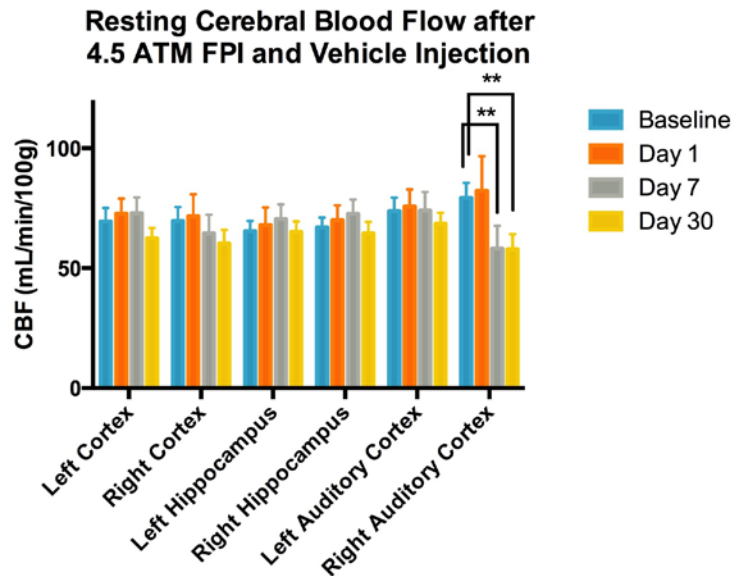


Figure 3. Resting Cerebral Blood Flow after Moderate Fluid Percussion Injury.

Two-way ANOVA revealed a significant main effect for time ( $p = 0.0028$ ) but not ROI. Bonferroni's multiple comparisons test revealed a significant decrease in CBF at the right auditory cortex from 79 mL/min/100g at baseline to 58 mL/min/100g on days 7 and 30 ( $n = 8$ , SE of diff = 6.8,  $DF = 126$ ).

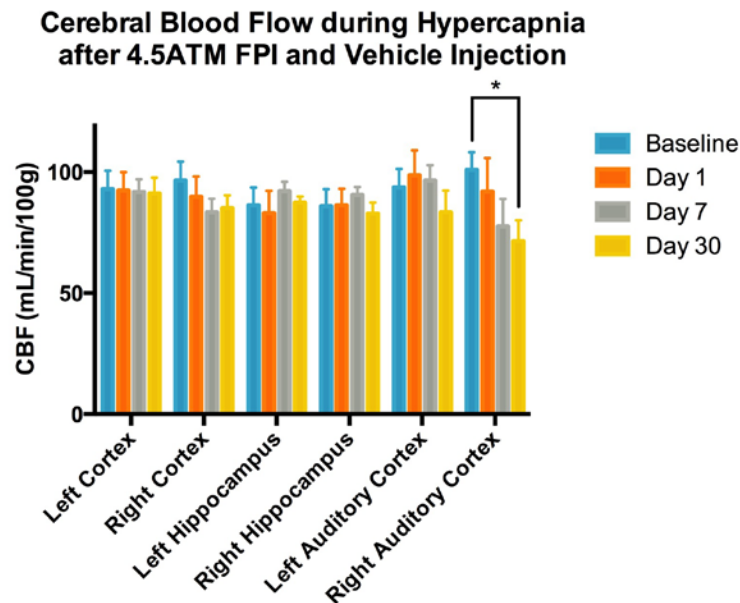


Figure 4. Cerebral Blood Flow with Hypercapnia after Moderate Fluid Percussion Injury. Two-way ANOVA revealed no significant main effect for ROI or time. Bonferroni's multiple comparisons analysis revealed a significant decrease in CBF at the right auditory cortex from 101 mL/min/100g at baseline to 71 mL/min/100g on day 30 (n=8, SE of diff= 10.9, DF= 126).

The trends in the percent change in CBF with hypercapnia appeared similar for both the right cortex and hippocampus compared to their respective contralateral ROI. The right auditory cortex showed an early decrease in CVR on day 1, followed by a mean increase on day 7, with return to values similar to the contralateral side by day 30, though none of these findings reached statistical significance (Figure 5). The box and whiskers plot in Figure 6 illustrates the percent change in CBF with hypercapnia varied considerably, most notably by day 7 in the right auditory cortex (Figure 6). When regional CVR values were normalized to the mean CVR value of the contralateral ROI, the overall variability appeared to be reduced, and the spread of CVR for the right

auditory cortex at days 7 and 30 following injury was more noticeable, though no values were found to be significant (Figure 7).

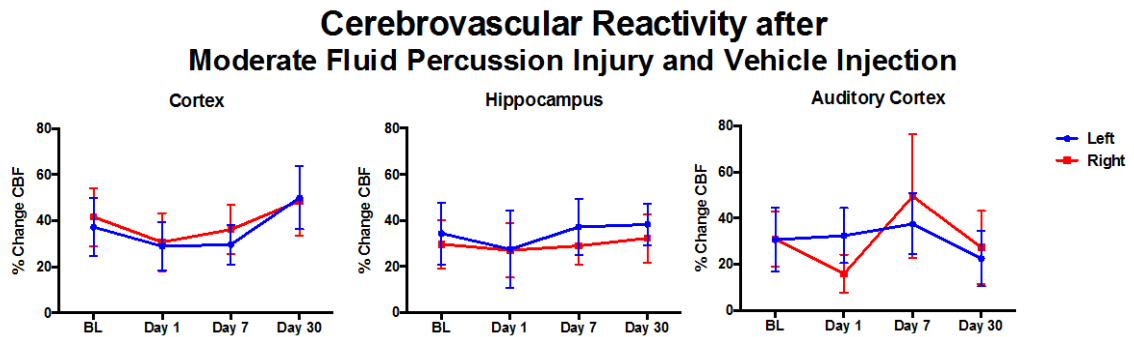


Figure 5. Cerebrovascular Reactivity after Moderate Fluid Percussion Injury and Vehicle Injection.

No significant differences were observed for hemisphere or time after injury for each of the three regions as assessed by repeated measures 2-way ANOVA (n=8 each). Error bars represent SEM.

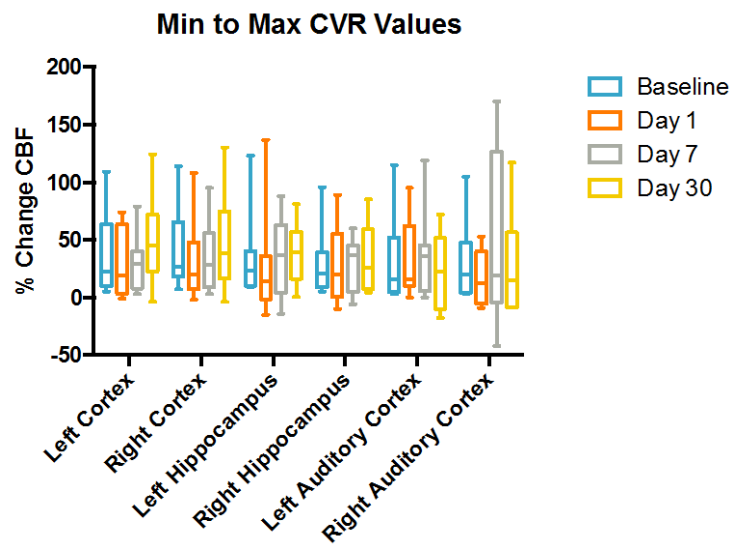


Figure 6. Min to Max Box and Whiskers Plot of CVR Values.

Box and whiskers plot depicts considerable spread in CVR values (n=8).

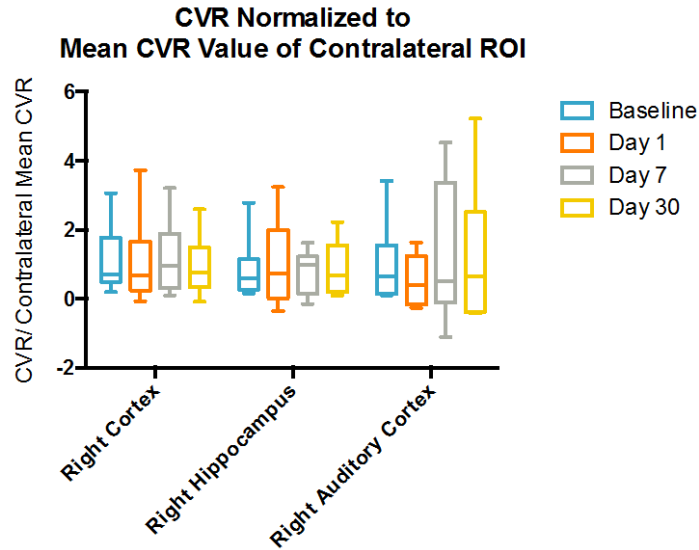


Figure 7. CVR Values Normalized to Mean of Contralateral ROI.

No significant differences were observed for ROI or time after injury assessed by repeated measures 2-way ANOVA (n=8 each). Whiskers represent min and max.

### Arterial Spin Labeling Assesses Sildenafil Effect After TBI

The deficits in CBF that were observed with medical air and hypercapnia in the right auditory cortex following TBI in rodents that received saline injection were not observed in rodents that received sildenafil treatment (Figs. 8 and 9). However, two-way ANOVA of CBF in right auditory cortex revealed no significant main effect of sildenafil compared to vehicle injection, both during medical air and hypercapnia (Figs. 10 and 11).

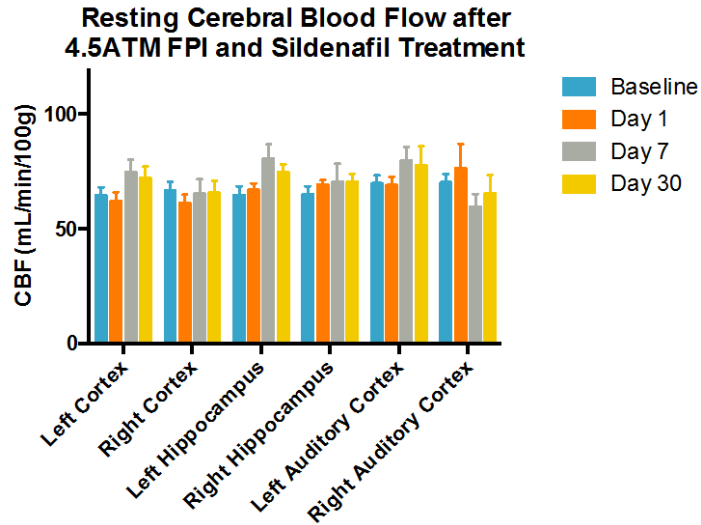


Figure 8. Resting Cerebral Blood Flow after Moderate Fluid Percussion Injury and Sildenafil Treatment.

Two-way ANOVA revealed no significant differences for region of interest or time after injury (n=7) and Bonferroni's multiple comparisons test revealed no differences in CBF after injury compared to baseline values for any ROI.

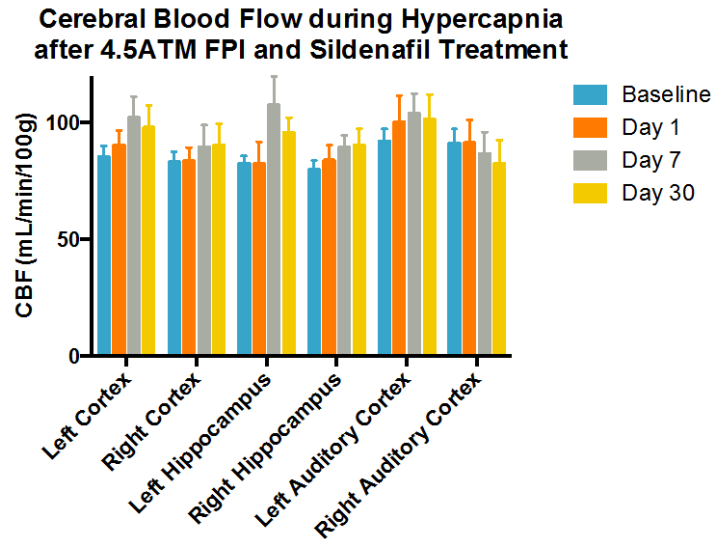


Figure 9. Cerebral Blood Flow with Hypercapnia after Moderate Fluid Percussion Injury and Sildenafil Treatment.

Two-way ANOVA revealed no significant differences for region of interest or time after injury (n=7) and Bonferroni's multiple comparisons test revealed no differences in CBF after injury compared to baseline values for any ROI.

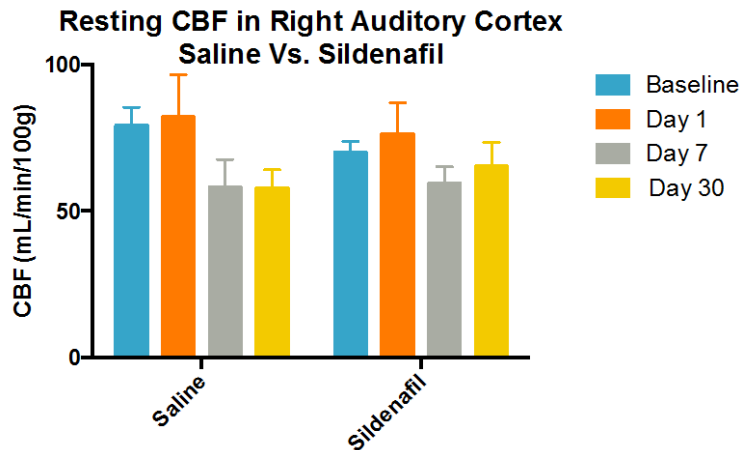


Figure 10. Effect of Sildenafil on Resting Cerebral Blood Flow in Right Auditory Cortex after TBI.

Two-way ANOVA revealed a significant main effect for time ( $p=0.019$ ) but not for treatment (saline  $n=8$ , sildenafil  $n=7$ ).

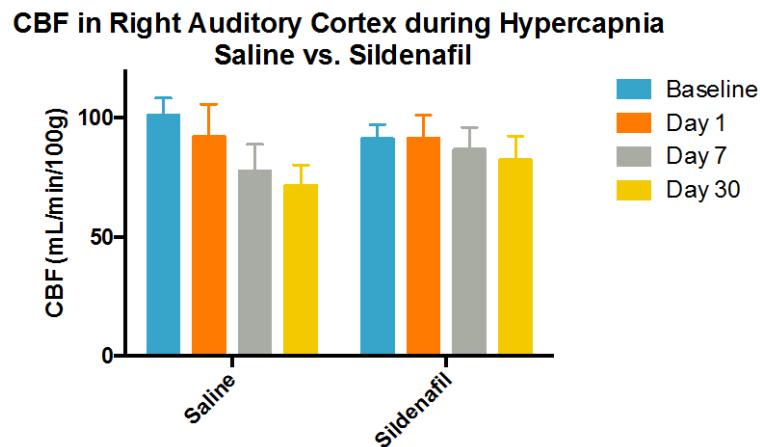


Figure 11. Effect of Sildenafil on Cerebral Blood Flow during Hypercapnia in Right Auditory Cortex after TBI.

The downward trend in CBF during hypercapnia after injury appears to be attenuated with sildenafil treatment, however, 2-way ANOVA revealed no significant main effects for time or treatment (saline  $n=8$ , sildenafil  $n=7$ ).



## Neurobehavioral Assessment after FPI

### *Neurologic Severity Score and Neurologic Severity Score-Revised*

Neurologic deficits were assessed with the neurologic severity score (NSS).

Ordinary 2-way ANOVA was utilized rather than repeated measures ANOVA due to absence of two values from dataset. Analysis revealed a significant main effect for group and time (see Fig. 12). Tukey's post-hoc revealed significant differences for FPI+Saline and FPI+Sildenafil compared to their respective baseline values at day 1 post injury only. Ordinary 2-way ANOVA of FPI groups revealed no significance difference between saline and sildenafil treatment. Similarly, no significant difference was observed for treatment using the NSS-R, though sildenafil appears to attenuate deficits (Fig. 13). Of note, mean deficits 1 day after TBI for the saline group measured less than one using the NSS, and measured 3 using the NSS-R.

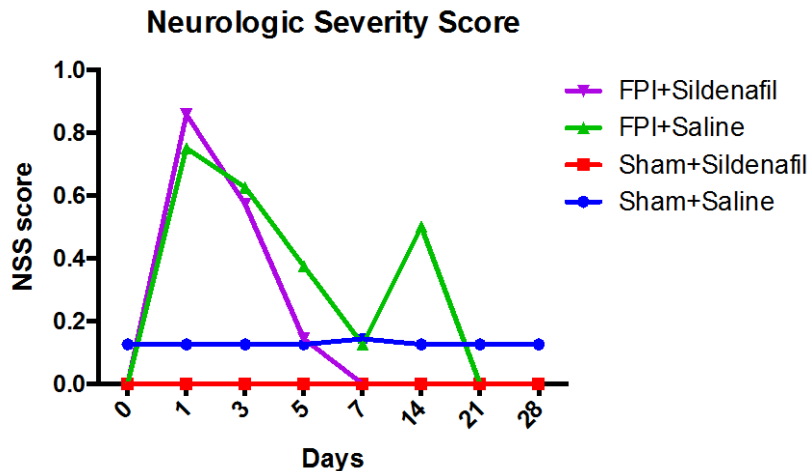


Figure 12. Temporal Profile of Neurologic Severity Score (NSS).

Ordinary 2-way ANOVA revealed significant main effects for group ( $p=0.011$ ) and time ( $p=0.011$ ). Tukey's multiple comparison test did not reveal a significant difference for FPI+saline versus FPI+sildenafil groups (sham+saline  $n=8$  with 1 missing value at day 7, sham+sildenafil  $n=9$  with one missing value at day 7, FPI+saline  $n=8$ , FPI+sildenafil  $n=7$ ).

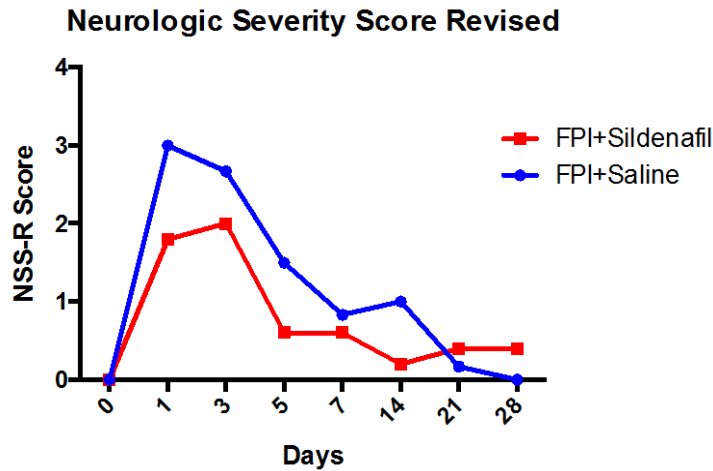


Figure 13. Temporal Profile of Neurologic Severity Score Revised (NSS-R) for the Treated and Control Groups.

Neurologic deficits after injury appear to be attenuated with sildenafil treatment, however, 2-way repeated measure ANOVA revealed no significant main effect for treatment (saline n=6, sildenafil n=5).

### *Open Field*

Open Field data was analyzed by two-way ANOVA. No significant differences in total distance traveled were observed for injury or treatment (data not shown). Two-way ANOVA revealed a significant main effect of injury on center time, with FPI groups showing increased center time compared to sham groups (Fig. 14). There was no main effect of treatment (Fig. 14).

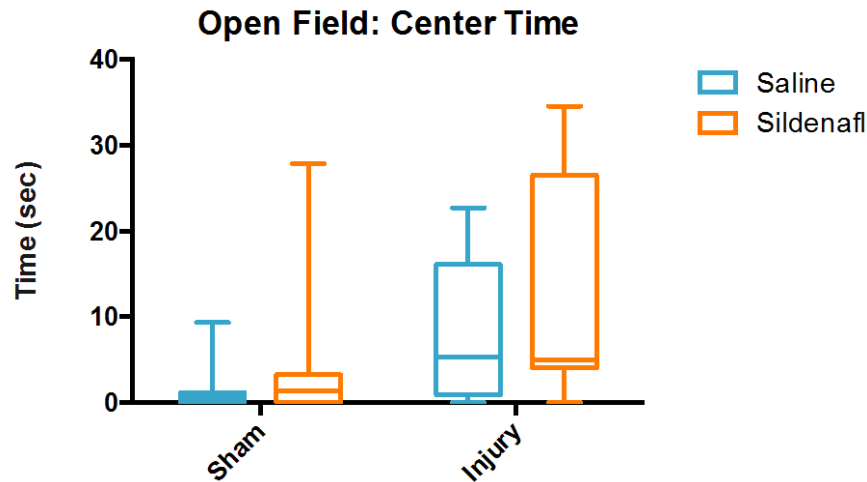


Figure 14. Time Spent in Center by Open Field Test.

Box and whiskers plot of min to max showing significantly increased time spent in center for injured groups compared to sham groups ( $p=0.0178$ ; sham+saline  $n=8$ , sham+sildenafil  $n=9$ , FPI+saline  $n=8$ , FPI+sildenafil  $n=7$ ).

### ***Rotorod***

The mean of the three trials on test day was analyzed by 2-way ANOVA. Due to malfunction of rotorod equipment, animal number per group was reduced (sham+saline  $n=8$ , sham+sildenafil  $n=9$ , FPI+saline  $n=4$ , FPI+sildenafil  $n=3$ ). No significant main effect of either injury or treatment was observed (data not shown).

### ***Water Maze***

Animals in all groups learned to find the platform rapidly during training days (Fig. 15). For this reason, repeated measures 2-way ANOVA was performed for trial one only, rather than the average of the 5 trials. No significant main effect was observed for either injury or treatment (Fig 16). 2-way ANOVA of time spent in prior quadrant on trial one of test day revealed no significant main effect of either injury or treatment.

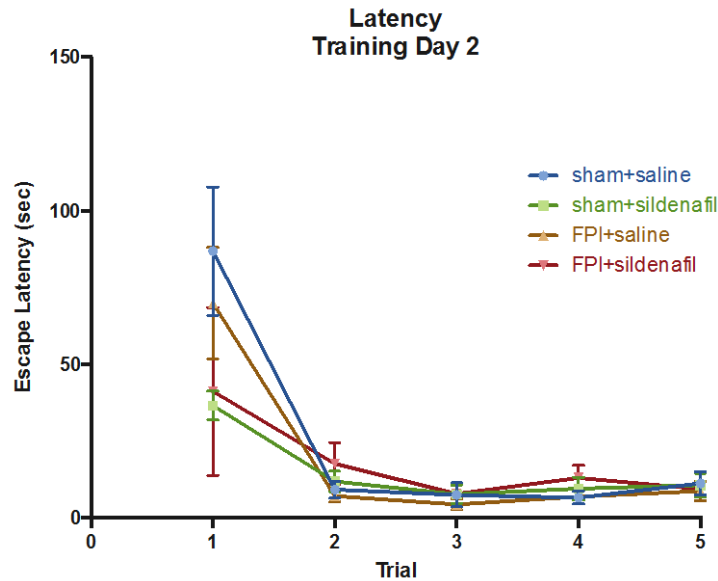


Figure 15. Water Maze Escape Latency during Training.  
Animals in all groups demonstrated ability to find platform rapidly across trials on the second day of training. Similar trends were observed on the other testing days. Error bars represent SEM.

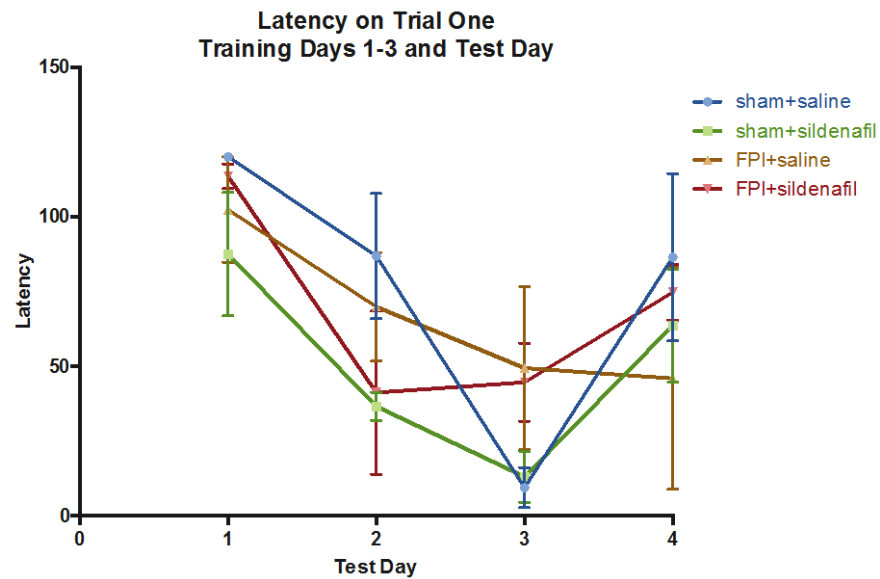


Figure 16. Water Maze Escape Latency across Training Days and Test Day.  
No clear trends were observed for latency to find platform on Trial 1 across training days 1-3, and on Trial 1 of the test day. Two-way repeated measures ANOVA revealed a main effect for time only ( $p < 0.001$ ). Error bars represent SEM.

## **Histologic Correlates**

The brain tissue of rats in the injured groups demonstrated increased GFAP and Iba-1 immunoreactivity in the ipsilateral auditory cortex. This region was distal from the area of impact, as the medial edge of the craniotomy site was located 1mm lateral to the sagittal suture. Qualitatively, the craniotomy site showed no cavitation, minimally enhanced GFAP immunoreactivity, and little to no enhanced Iba-1 immunoreactivity. (Fig. 17). At the site of the enhanced Iba-1 immunoreactivity, examination at 20X revealed swollen cell bodies with thickened and shortened processes, consistent with local microglial activation (Fig. 18). GFAP immunolabeling also demonstrated increased astrogliosis in the ipsilateral cortex and external capsule (Fig. 19). Iba-1 immunolabeling demonstrated microglial activation in the ipsilateral cortex, external capsule, and hippocampus (Fig. 20). No regional increase in RECA-1 immunolabeling was appreciated by visual inspection of the scanned tissue. Analysis of percent area of RECA-1 revealed significantly increased immunoreactivity one month after injury compared to sham groups for the ipsilateral auditory cortex only (Fig. 21). No main effect of treatment was observed for any of the four regions with GFAP, Iba-1, or RECA-1.

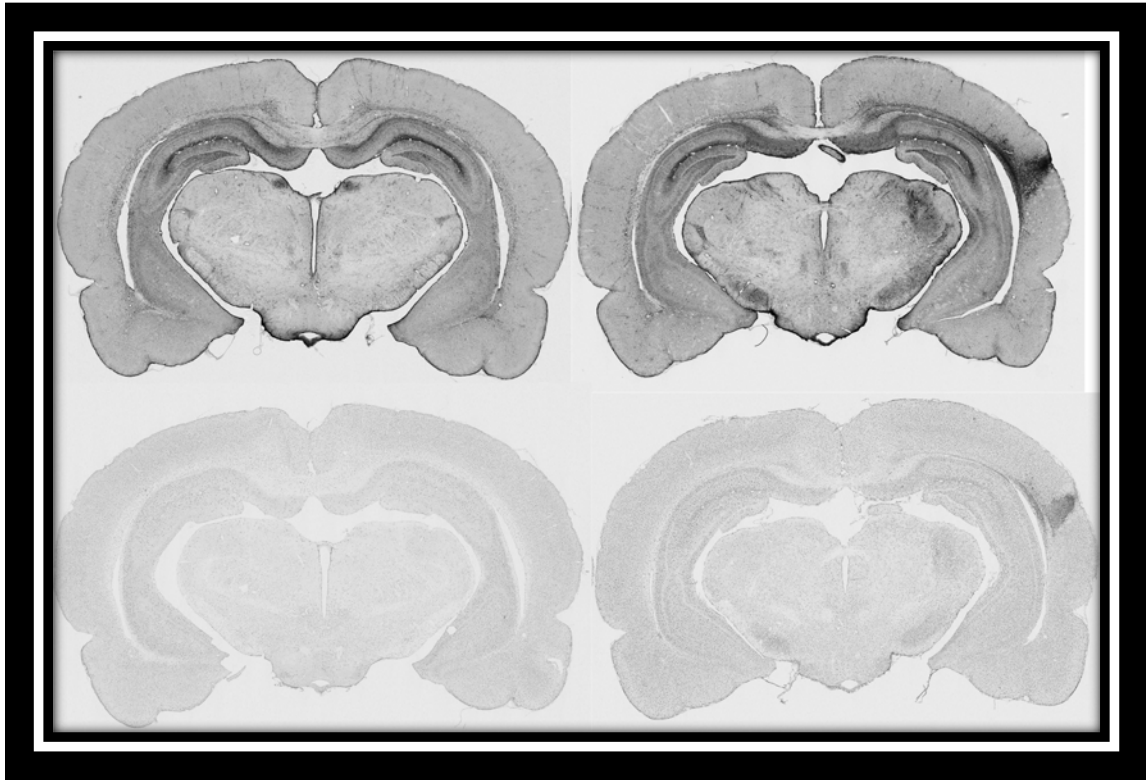


Figure 17. Representative Images of GFAP and Iba-1 Immunoreactivity.

One month after sham-FPI (left column), histology shows uniform GFAP (top row) and Iba-1 (bottom row) immunoreactivity. Tissue sections from animals injured with an FPI of 4.5 atm (right column) show very high immunoreactivity of GFAP (top) and Iba-1 (bottom) in the ipsilateral auditory cortex and external capsule one month after injury.

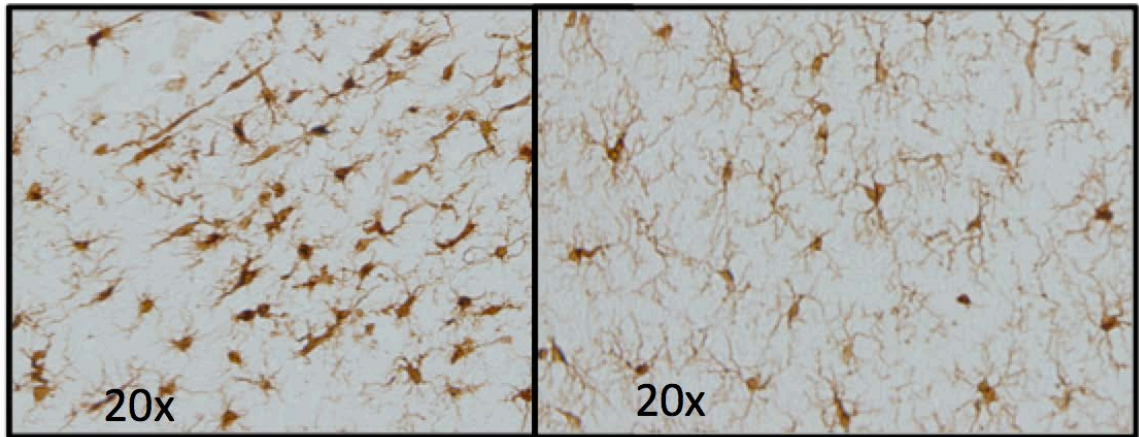


Figure 18. Representative Images of Iba-1 Morphology.

One month after fluid percussion injury, microglial activation is apparent in the auditory cortex ipsilateral to the side of injury (left) compared to typical ramified, resting microglia in uninjured tissue (right).

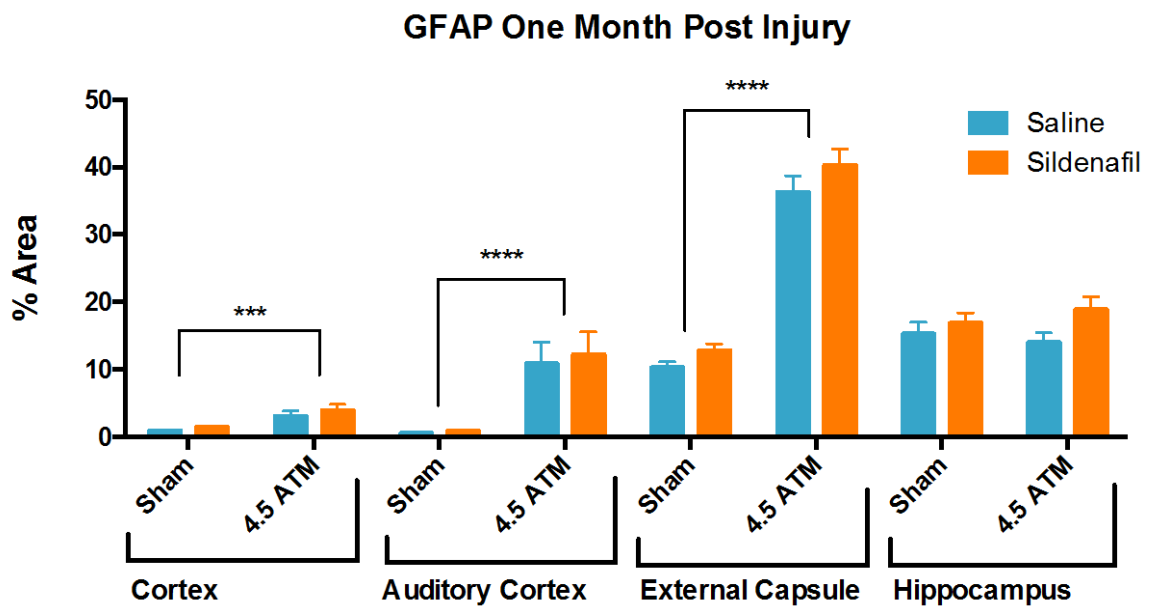


Figure 19. Increased GFAP Immunoreactivity after Injury.

Two-way ANOVA revealed a significant main effect of injury, with an increase in GFAP immunoreactivity in the ipsilateral cortex ( $p=0.0003$ ), auditory cortex ( $p<0.0001$ ), and external capsule ( $p<0.0001$ ) one month after injury. No significant increase in GFAP immunoreactivity was detected in the ipsilateral hippocampus. No significant effect of treatment was detected for any region.

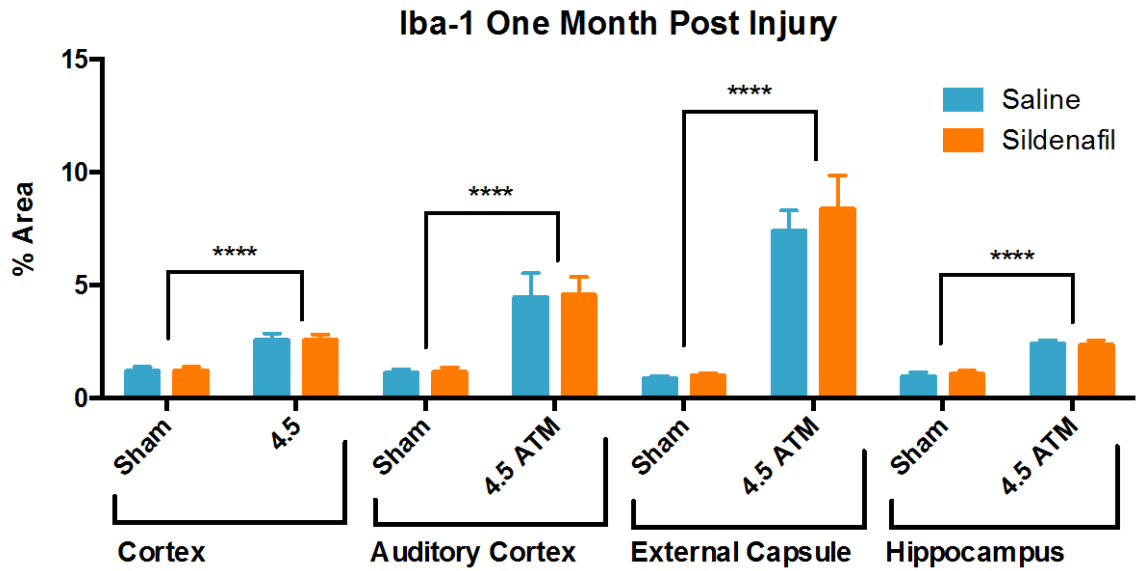


Figure 20. Increased Iba-1 Immunoreactivity after Injury.

Two-way ANOVA revealed a significant main effect of injury, with an increase in Iba-1 immunoreactivity in the ipsilateral cortex ( $p < 0.0001$ ), auditory cortex ( $p < 0.0001$ ), and external capsule ( $p < 0.0001$ ), and hippocampus ( $p < 0.0001$ ) one month after injury. No significant effect of treatment was detected for any region.



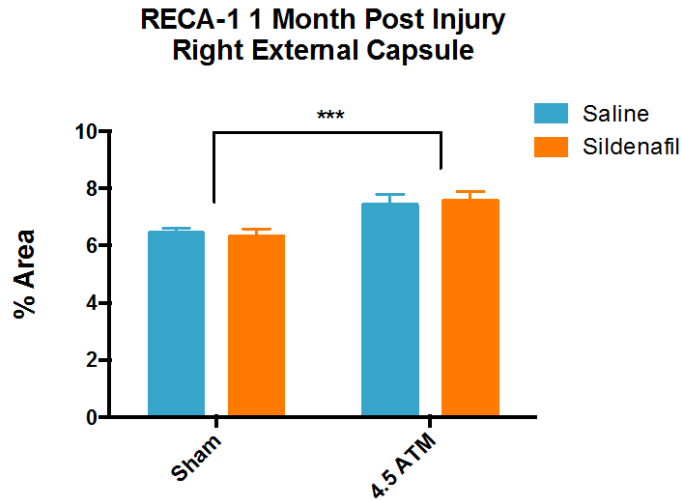


Figure 21. RECA-1 Immunolabeling of Vasculature 1 Month after Injury.

One month after surgery, there was a significant increase in the percent area of RECA-1 immunoreactivity in the ipsilateral external capsule compared to sham ( $p=0.0006$ , sham+saline  $n=8$ , FPI+saline  $n=8$ , sham+sildenafil  $n=9$ , FPI+sildenafil  $n=7$ ). No significant effect of sildenafil treatment was observed.

### AIM 3: THE RELATION BETWEEN CEREBROVASCULAR AND AXONAL INJURY

Analysis of diffusion tensor imaging was completed using five regions of interest (ROIs) for white matter: corpus callosum, the left and right medial segments of the external capsule, and the left and right lateral segments of the external capsule. Analysis of grey matter was completed using six ROIs: left and right hippocampi, left and right lateral cortex, and left and right medial cortex (Fig. 22). The external capsule was divided into medial and lateral segments due to different orientation of fibers in these regions, which would confound DTI results if analyzed as a single ROI.

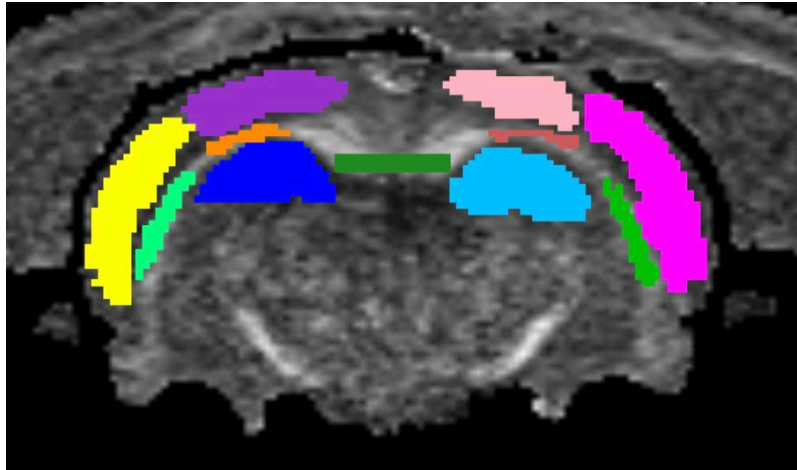


Figure 22. Regions of Interest Included in Diffusion Tensor Imaging Analysis.

Yellow: Left lateral cortex, purple: left medial cortex, peach: right medial cortex, pink: right lateral cortex, bright green: left lateral external capsule, orange: left medial external capsule, forest green: corpus callosum, brown: right medial external capsule, green: right lateral external capsule, dark blue: left hippocampus, sky blue: right hippocampus.

Analysis of mean diffusivity in white matter ROIs revealed a significant increase in the medial and lateral segments of the ipsilateral external capsule one day after injury (Fig. 23). The effect of sildenafil treatment was then assessed for these two ROIs.

Sildenafil significantly reduced the increase in MD observed at day 1 post injury for both ROIs (Fig. 24-25).

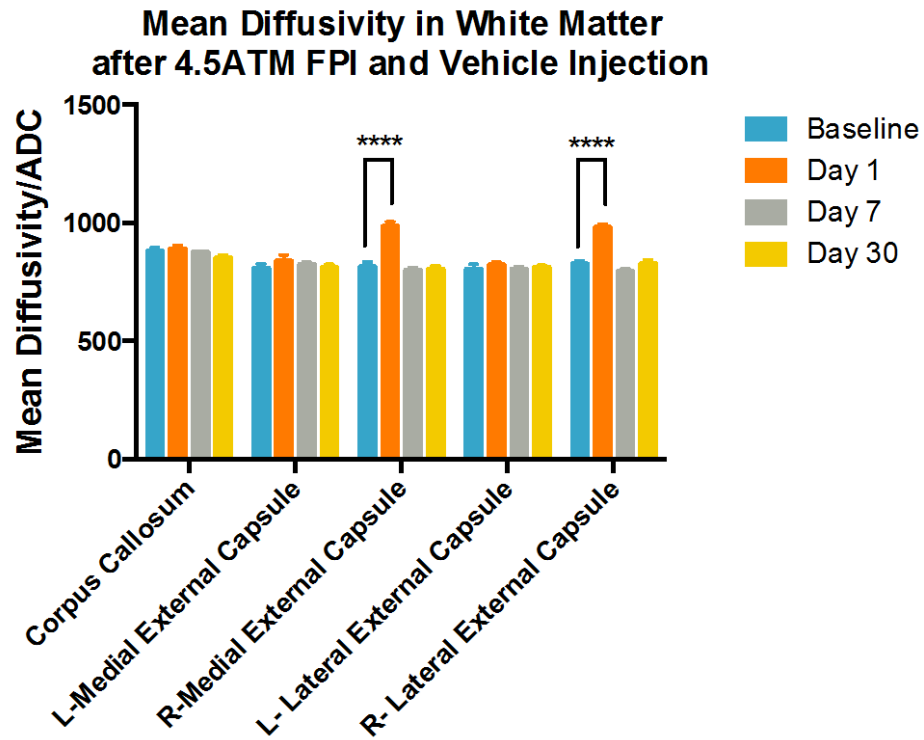


Figure 23. Mean Diffusivity of White Matter.

Two-way repeated measures ANOVA revealed significant main effect for ROI, time, and interaction (each  $p < 0.0001$ ). Bonferroni's multiple comparisons test revealed a significant increase in mean diffusivity of the right medial and lateral external capsule one day post injury. Error bars represent SEM.

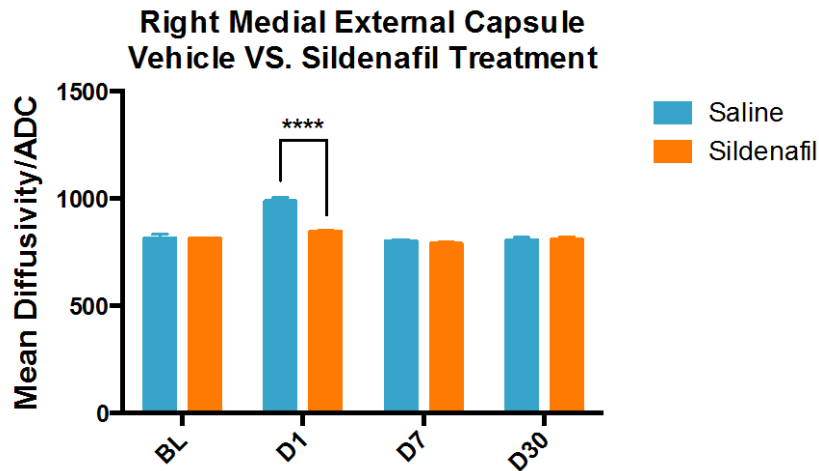


Figure 24. Mean Diffusivity of Medial External Capsule.

Two-way repeated measures ANOVA revealed significant main effect for time ( $p < 0.0001$ ), treatment ( $p = 0.0024$ ), and interaction ( $p < 0.0001$ ). Sidak's multiple comparisons test revealed a significant difference in mean diffusivity one day post injury with sildenafil treatment (each  $p < 0.0001$ ). Error bars represent SEM.

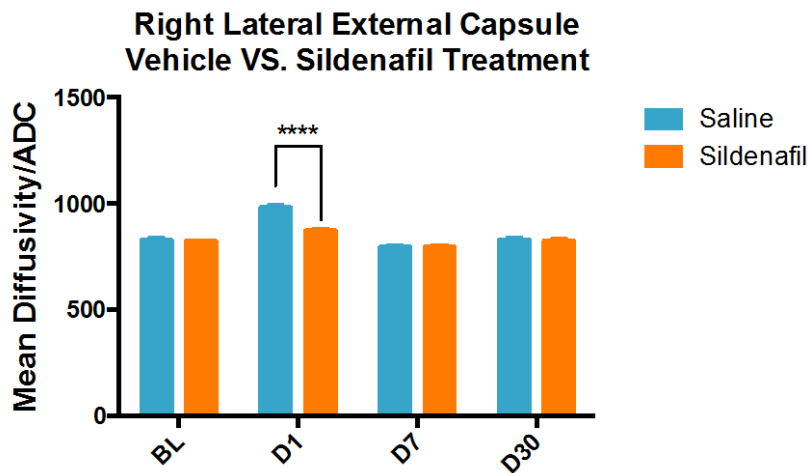


Figure 25. Mean Diffusivity of Lateral External Capsule.

Two-way repeated measures ANOVA revealed significant main effect for time ( $p < 0.0001$ ), treatment ( $p = 0.0040$ ), and interaction ( $p < 0.0001$ ). Sidak's multiple comparisons test revealed a significant difference in mean diffusivity one day post injury with sildenafil treatment (each  $p < 0.0001$ ). Error bars represent SEM.

Analysis of mean diffusivity in grey matter ROIs revealed a significant increase in the medial and lateral segments of the ipsilateral cortex one day after injury (Fig. 26). The effect of sildenafil treatment was then assessed for these two ROIs. Sildenafil significantly reduced the increase in MD observed at day 1 post injury for both ROIs, however there was an increase in MD in the lateral cortex on day 7 in the sildenafil treated group (Fig. 27-28).

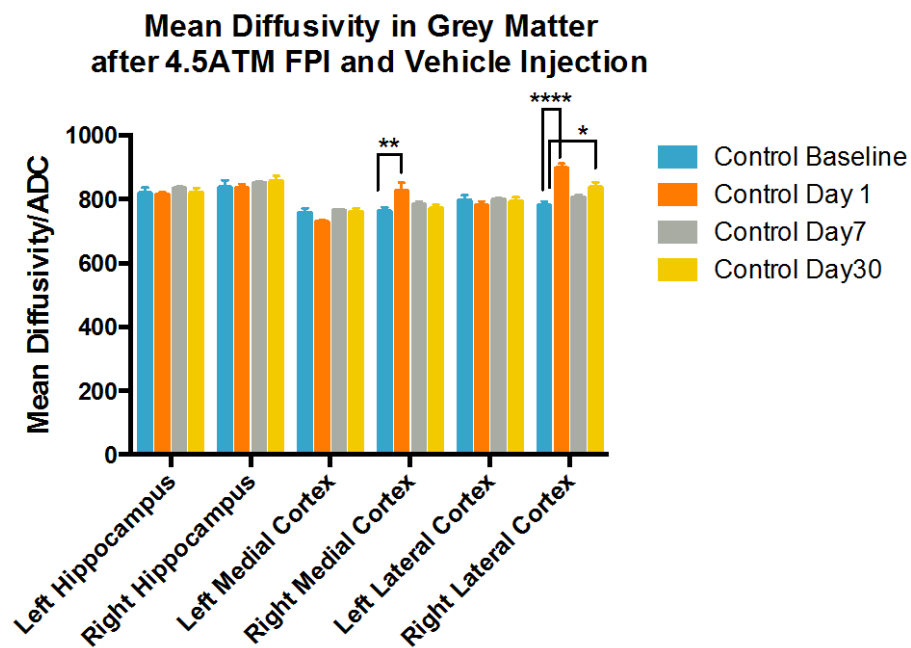


Figure 26. Mean Diffusivity of Grey Matter.

Two-way repeated measures ANOVA revealed significant main effect for ROI and interaction (each  $p < 0.0001$ ) but not for time ( $p = 0.0568$ ). Bonferroni's multiple comparisons test revealed a significant increase in mean diffusivity of the right medial cortex one day post injury and of the right lateral cortex one day and one month post injury compared to baseline. Error bars represent SEM.

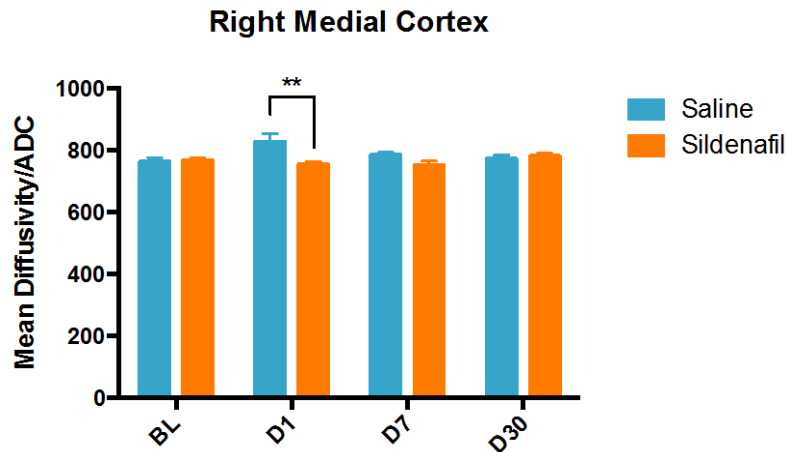


Figure 27. Mean Diffusivity of Medial Cortex.

Two-way repeated measures ANOVA revealed significant main effect for treatment ( $p=0.0028$ ) and interaction ( $p=0.0445$ ). Sidak's multiple comparisons test revealed a significant difference in mean diffusivity one day post injury with sildenafil treatment. Error bars represent SEM.

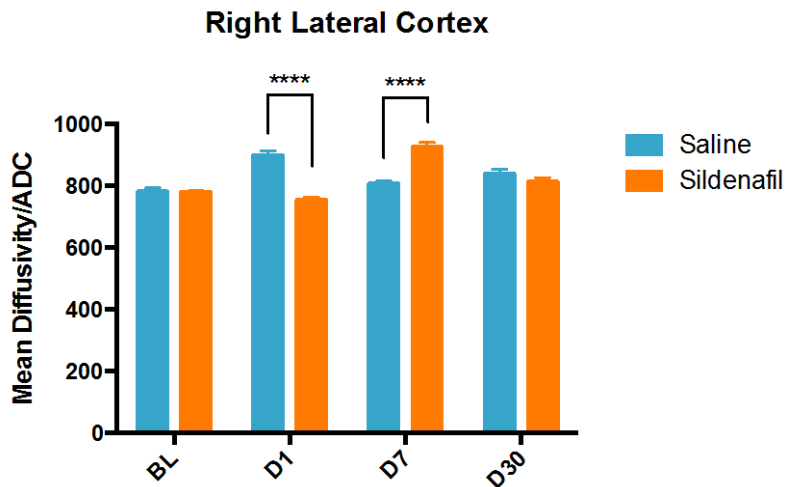


Figure 28. Mean Diffusivity of Lateral Cortex.

Two-way repeated measures ANOVA revealed significant main effect for time ( $p<0.0001$ ) and interaction ( $p<0.0001$ ). Sidak's multiple comparisons test revealed a significant difference in mean diffusivity days 1 and 7 post injury comparing treatment groups, with opposing effects on these days. Error bars represent SEM.

Analysis of fractional anisotropy (FA) in white matter ROIs revealed a significant decrease in the ipsilateral lateral segment of the external capsule on days 1, 7, and 30 after injury compared to baseline, and on day 30 in the contralateral medial segment (Fig. 29). The effect of sildenafil treatment was then assessed for the ipsilateral external capsule, in consistency with previous analysis of MD. The sildenafil treated group demonstrated statistically significant greater FA values than saline treated group at day 30 post injury (Fig. 30).

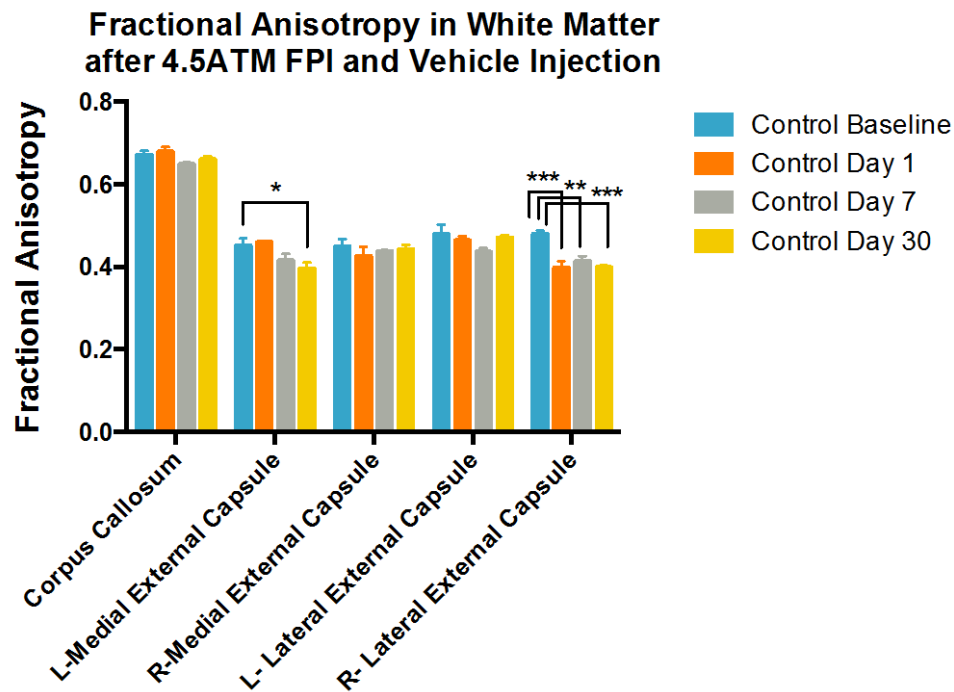


Figure 29. Fractional Anisotropy in White Matter.

Two-way repeated measures ANOVA revealed significant main effect for ROI ( $p < 0.0001$ ), time ( $p = 0.0002$ ) and interaction ( $p = 0.0122$ ). Bonferroni's multiple comparisons test revealed a significant difference in fractional anisotropy in the contralateral medial external capsule day 30 compared to baseline and in the ipsilateral lateral external capsule on days 1, 7, and 30 compared to baseline. Error bars represent SEM.

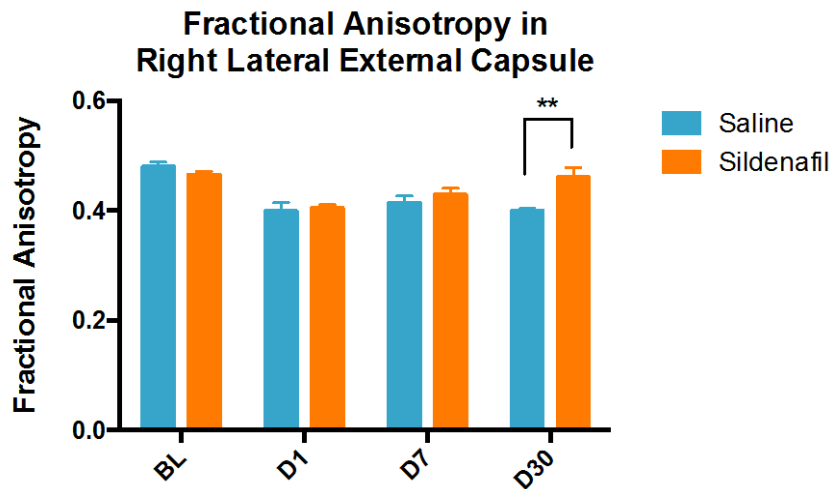


Figure 30. Fractional Anisotropy of Lateral External Capsule.

Two-way repeated measures ANOVA revealed significant main effect for time ( $p < 0.0001$ ), treatment ( $p = 0.0275$ ), and interaction ( $p = 0.0233$ ). Sidak's multiple comparisons test revealed a significant increase in fractional anisotropy day 30 post injury with sildenafil treatment. Error bars represent SEM.

FA values in grey matter ROIs revealed a significant main effect for ROI ( $p = 0.0088$ ) and time (0.0042). Bonferroni's multiple comparisons test did not reveal significant differences between baseline and post-injury FA values for any ROI and therefore no ROI was selected for assessing the sildenafil effect (data not shown).

Analysis of axial diffusivity (AD) in white matter ROIs revealed significant differences in the ipsilateral medial segment of the external capsule, with an increase on day 1 and a decrease on day 30 post injury. In the ipsilateral lateral segment, there was a significant increase on day 1 and decrease on days 7 and 30 compared to baseline (Fig. 31). The effect of sildenafil treatment was then assessed for these two ROIs. There was no significant main effect of treatment for the medial segment of the external capsule, though post-hoc analysis revealed a significant difference in saline versus sildenafil



treated animals on day 7, with sildenafil treated animals showing lower values (data not shown). Similarly, there was no significant main effect of treatment for the lateral segment of the external capsule, though post-hoc analysis revealed a significant difference in saline versus sildenafil treated animals on day 1, with sildenafil treated animals showing lower FA values.

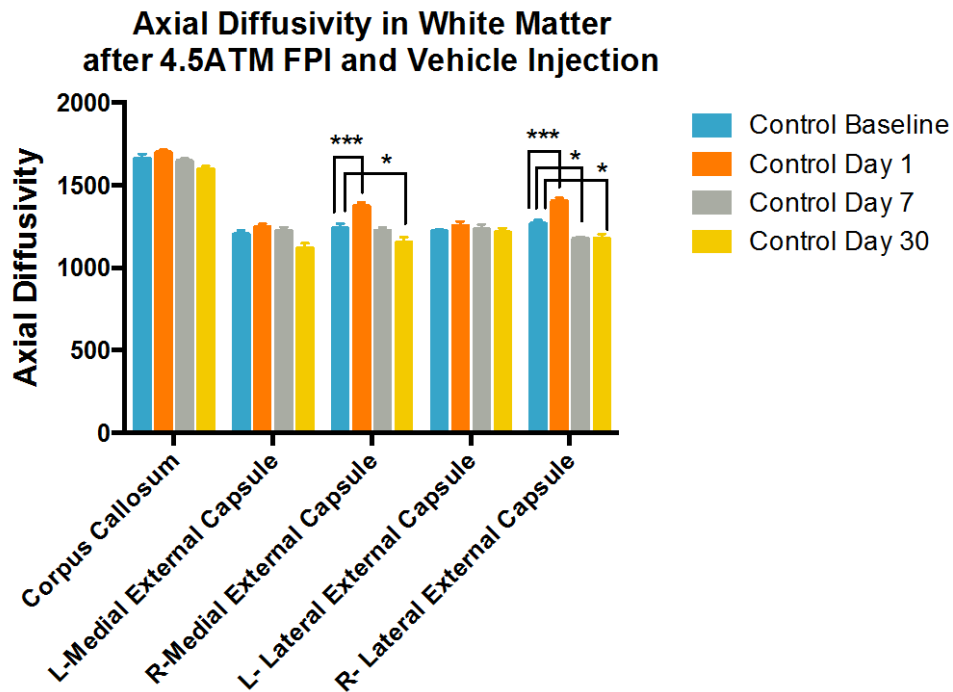


Figure 31. Axial Diffusivity in White Matter.

Two-way repeated measures ANOVA revealed a significant main effect for ROI ( $p < 0.0001$ ), time ( $p < 0.001$ ) and interaction ( $p = 0.0010$ ). Bonferroni's multiple comparisons test revealed a significant difference in axial diffusivity in the ipsilateral medial external capsule on day 1 (increased) and day 30 (decreased) compared to baseline and in the ipsilateral lateral external capsule on days 1 (increased), 7 (decreased), and 30 (decreased) compared to baseline. Error bars represent SEM.

Analysis of AD values in grey matter ROIs revealed a significant main effect for ROI ( $p = 0.0001$ ) but not for the time or interaction of factors. For each ROI, no significant

changes from baseline values were observed, thus no ROI was selected to assess the sildenafil effect (data not shown).

Analysis of radial diffusivity (RD) in white matter ROIs revealed a significant increase in the ipsilateral lateral external capsule on day 1 post injury compared to baseline (Fig. 32). The effect of sildenafil treatment was then assessed for this ROI, which showed a significant main effect of time, treatment, and interaction. Sildenafil treated animals demonstrated statistically significant lower RD values on days 1 and 30 post injury compared to saline treated animals (Fig. 33).

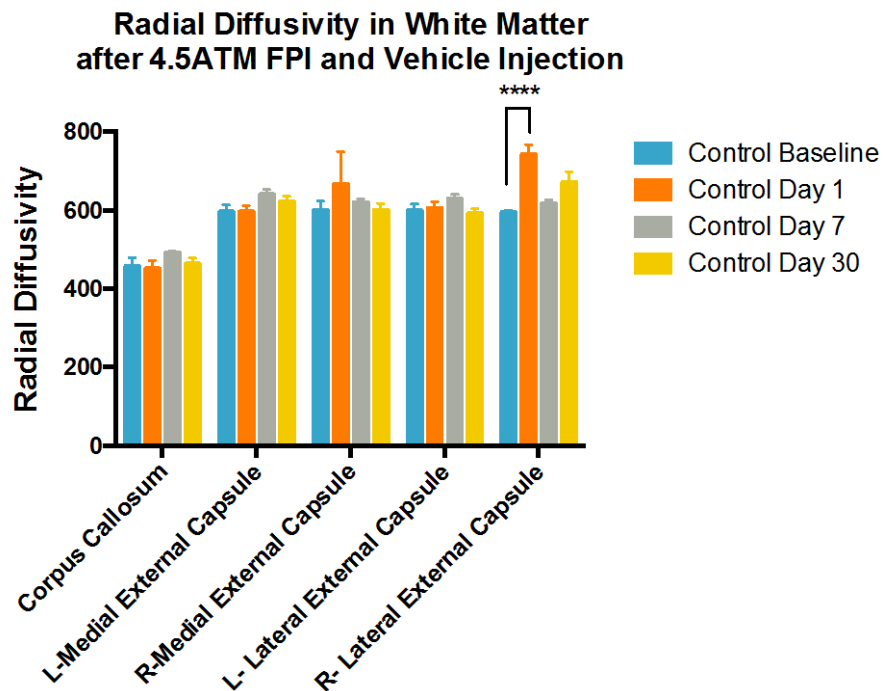


Figure 32. Radial Diffusivity in White Matter.

Two-way repeated measures ANOVA revealed a significant main effect for ROI ( $p < 0.0001$ ), time ( $p = 0.0375$ ) and interaction ( $p = 0.0245$ ). Bonferroni's multiple comparisons test revealed a significant difference in radial diffusivity in the ipsilateral lateral external capsule day 1 compared to baseline. Error bars represent SEM.

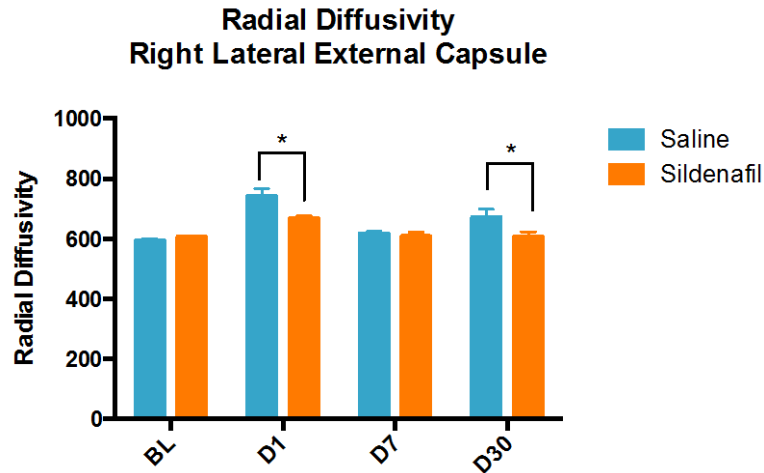


Figure 33. Radial Diffusivity of Lateral External Capsule.

Two-way repeated measures ANOVA revealed a significant main effect for time ( $p < 0.0001$ ), treatment ( $p = 0.0304$ ) and interaction ( $p = 0.0200$ ). Sidak's multiple comparisons test revealed a significant difference in radial diffusivity in sildenafil treated animals compared to saline days 1 and 30 post injury. Error bars represent SEM.

Analysis of RD in grey matter ROIs revealed a significant increase in the ipsilateral medial cortex on day 1 post injury compared to baseline and on days 1, 7, and 30 in the ipsilateral lateral cortex (Fig. 34). The effect of sildenafil treatment was then assessed for these ROIs. The right medial cortex showed a significant main effect for treatment and interaction, with post-hoc showing a significant reduction in RD day 1 post injury with sildenafil treatment (Fig. 35). The right lateral cortex showed a significant main effect for time and interaction but not treatment. Post-hoc revealed significant differences between saline and sildenafil treated animals, with the sildenafil group showing lesser values on day 1 and greater values on day 7 (Fig. 36).

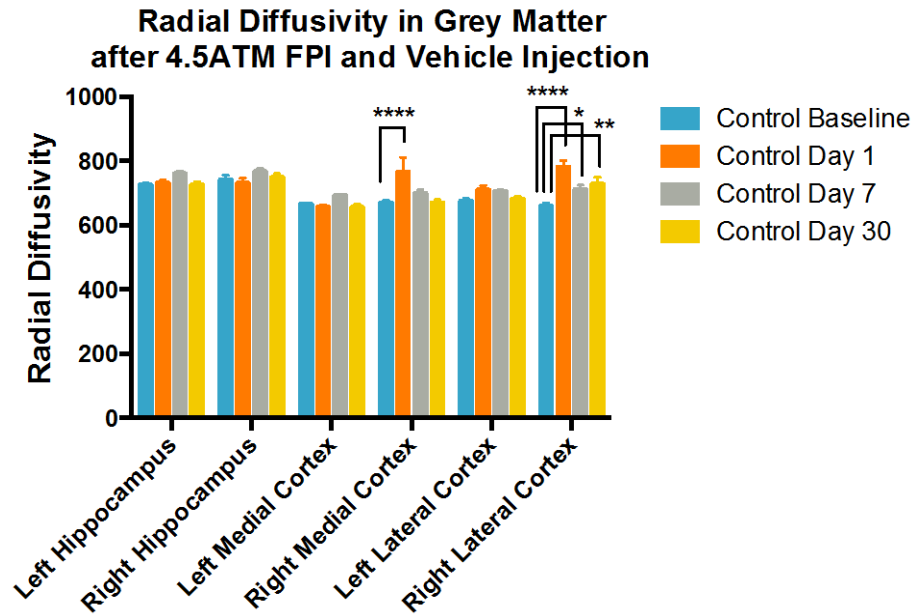


Figure 34. Radial Diffusivity in Grey Matter.

Two-way repeated measures ANOVA revealed a significant main effect for ROI, time, and interaction (each  $p < 0.0001$ ). Bonferroni's multiple comparisons test revealed a significant increase in radial diffusivity in the ipsilateral medial cortex day 1 compared to baseline and in the ipsilateral lateral cortex on days 1, 7, and 30. Error bars represent SEM.

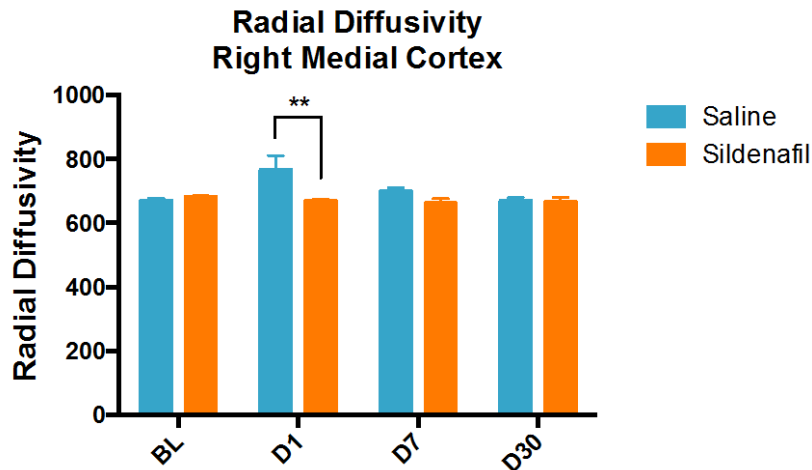


Figure 35. Radial Diffusivity of Right Medial Cortex.

Two-way repeated measures ANOVA revealed a significant main effect for treatment ( $p = 0.0245$ ) and interaction ( $p = 0.0499$ ). Sidak's multiple comparisons test revealed a significant difference in radial diffusivity in sildenafil treated animals compared to saline day 1 post injury. Error bars represent SEM.

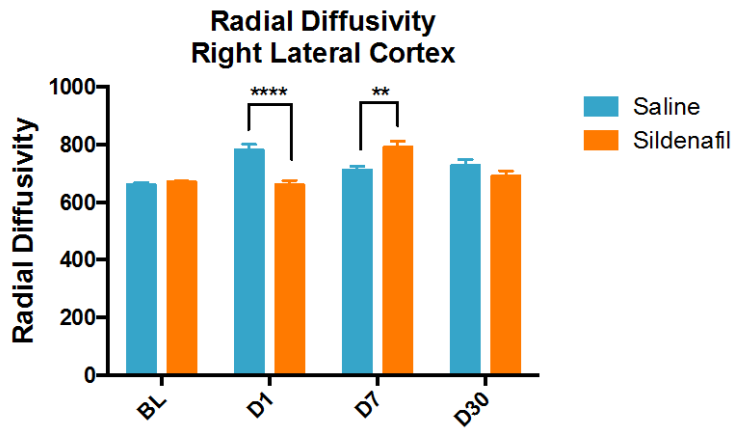


Figure 36. Radial Diffusivity of Right Lateral Cortex.

Two-way repeated measures ANOVA revealed a significant main effect for time and interaction (each  $p < 0.0001$ ). Sidak's multiple comparisons test revealed significant differences in radial diffusivity in sildenafil treated animals compared to saline, with a decrease on day 1 and an increase on day 7. Error bars represent SEM.

Results of histology and CBF in the right auditory cortex, which corresponds to right lateral cortex DTI data, as well as results for right external capsule, are summarized in Tables 2 and 3, respectively. Additionally, the relationship between resting CBF and DTI parameters in the right auditory cortex were investigated by plotting those values for each animal in the FPI + saline group, summarized graphically in Table 4. There was a negative correlation of resting CBF and FA of the right auditory cortex on day 7 after injury. However, there were no clear temporal trends between resting CBF and either MD, FA, AD, or RD of the right auditory cortex. Assessment of resting CBF and the adjacent white matter in the right external capsule revealed a positive correlation day 7 after injury, however no other temporal trends were observed (Table 5). False discovery

rate (FDR) correction for these 24 comparisons resulted in loss of significance of the two significant observations from Spearman's analysis.

Right Auditory Cortex							
Assessment		Saline after Injury vs. Baseline		Sildenafil after Injury vs. Baseline		Sildenafil Effect after Injury vs. Saline	Notes/ Interpretation (note statistical significance)
Day Post Injury		1	7	30	1	7	30
GFAP				↑		↑	No appreciable effect
Iba-1			↑			↑	No appreciable effect
Resting CBF		-	↓	↓	-	-	Sildenafil effect not statistically sig.
CBF on 5% CO2		-	-	↓	-	-	Sildenafil effect not statistically sig.
MD		↑	-	↑	-	-	Sildenafil reverses the MD increase d1 and d30 (with paradoxical increase d7)
FA		-	-	-	-	-	
AD		-	-	-	↑	-	
RD		↑	↑	↑	-	↑	Sildenafil reverses the increase in RD d1 (significant), increases RD d7 (sig.), and attenuates the increase d30 (not sig.)

Table 2. Summary of Histologic and MRI Findings in Right Auditory Cortex after TBI.  
The table summarizes the effects of injury and sildenafil treatment on GFAP, Iba-1, Cerebral Blood Flow (CBF) as measured by arterial spin labeling, and Mean Diffusivity (MD), Fractional Anisotropy (FA), Axial Diffusivity (AD), and Radial Diffusivity (RD) by diffusion tensor imaging.

Right External Capsule									
		Saline after Injury vs. Baseline			Sildenafil after Injury vs. Baseline			Sildenafil Effect after Injury vs. Saline	Notes/ Interpretation (note statistical significance)
Assessment	Day Post Injury	1	7	30	1	7	30		
GFAP				↑			↑	No appreciable effect	
Iba-1				↑			↑	No appreciable effect	
RECA-1				↑			↑	No appreciable effect	
MD: Med Seg		↑	-	-	-	-	-	↓	
MD: Lat Seg		↑	-	-	↑	-	-	↓	Sildenafil reversed the MD increase
FA: Med Seg		-	-	-	↓	↓	↓		Sildenafil attenuated the MD increase
FA: Lat Seg		↓	↓	↓	↓	-	-	↑	Sildenafil reversed the FA decrease d7 (direct effect not sig.) and d30 (significant)
AD: Med Seg		↑	-	↓	↓	↓	↓	↓	Sildenafil decreased FA d7 (significant) and reversed the increase on d1 (not significant)
AD: Lat Seg		↑	↓	-	↓	-	-	↓	Sildenafil reversed the increase in FA d1 (significant)
RD: Med Seg		-	-	-	-	-	-		Sildenafil attenuated the increase in RD d1 (sig.) and decreased RD d30 (sig. effect but not significantly below BL)
RD: Lat Seg		↑	-	-	↑	-	-	↓	

Table 3. Summary of Histologic and MRI Findings in Right External Capsule after TBI.

The table summarizes the effects of injury and sildenafil treatment on GFAP, Iba-1, Cerebral Blood Flow (CBF) as measured by arterial spin labeling, and Mean Diffusivity (MD), Fractional Anisotropy (FA), Axial Diffusivity (AD), and Radial Diffusivity (RD) by diffusion tensor imaging.



Table 4. Correlation of Resting CBF and DTI Parameters of Injured Grey Matter.

The table depicts changes in resting CBF versus mean diffusivity, fractional anisotropy, axial diffusivity, and radial diffusivity in the right auditory cortex in each animal after injury. Animals received saline injection only. Spearman's Correlation revealed a significant association for resting CBF vs. FA at day 7 ( $r = -0.8095$ , two-tailed  $p$ -value = 0.0218,  $n = 8$ ). This effect lost significance after FDR correction for multiple comparisons (24  $p$ -values included).

# Resting CBF and Diffusion Rt Aud Cx

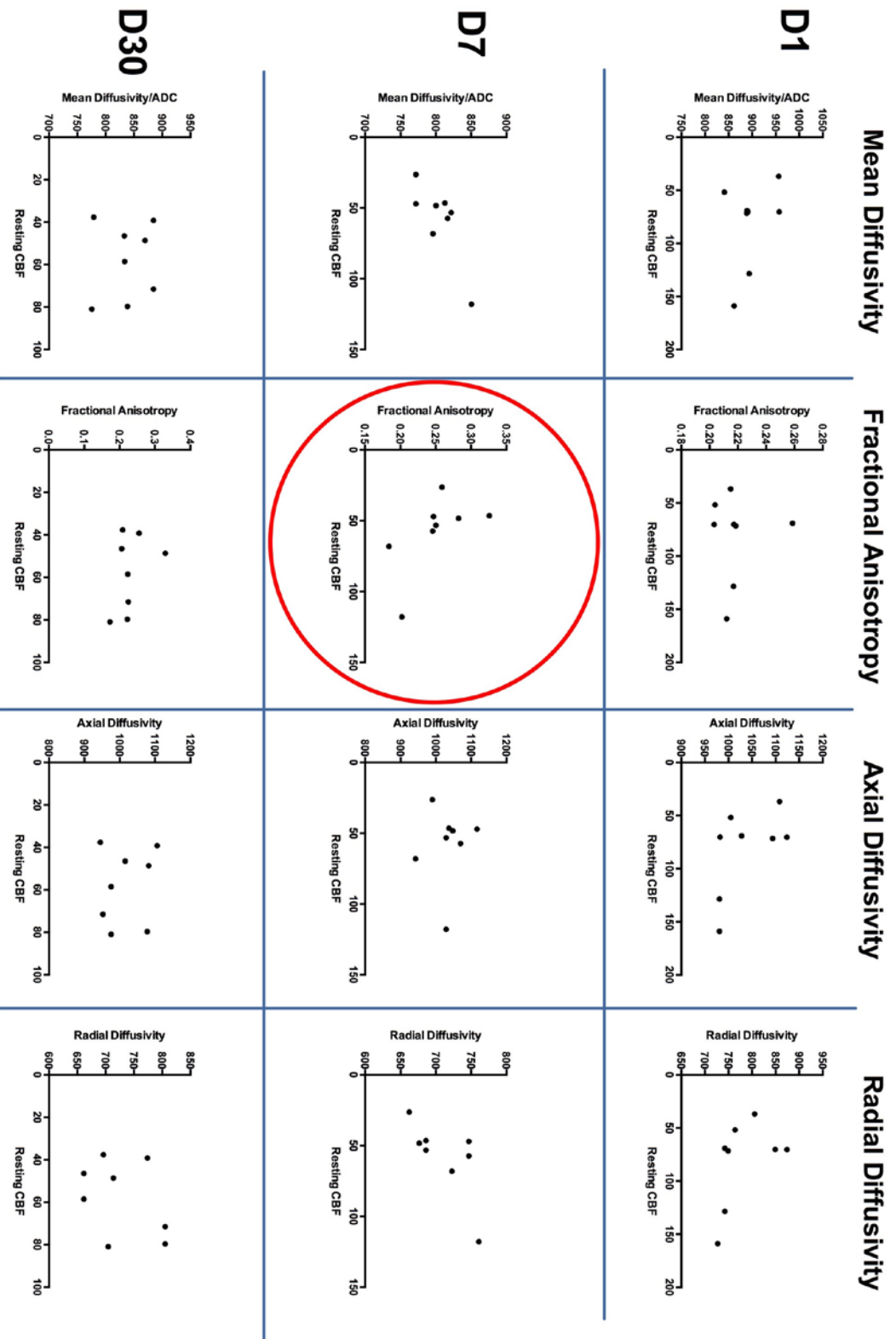
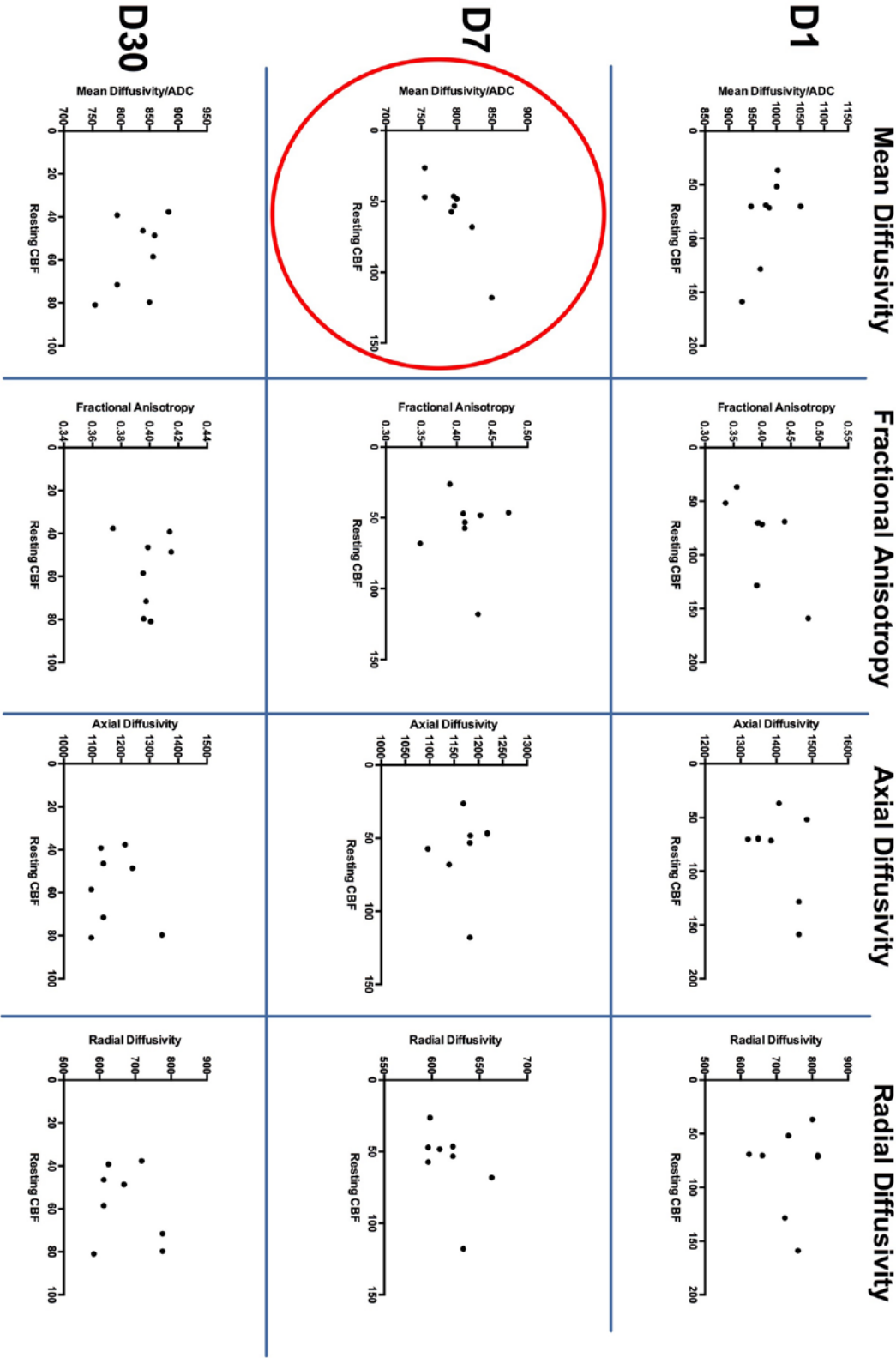


Table 5. Correlation of Resting CBF in Injured Cortex and DTI Parameters of Adjacent White Matter.

The table depicts changes in mean diffusivity, fractional anisotropy, axial diffusivity, and radial diffusivity in the right external capsule versus resting CBF of the auditory cortex in each animal after injury. Animals received saline injection only. Spearman's Correlation revealed a significant association for resting CBF vs. MD at day 7 ( $r = +0.7665$ , two-tailed  $p$ -value = 0.0324,  $n = 8$ ). This effect lost significance after FDR correction for multiple comparisons (24  $p$ -values included).

Resting CBF of Rt Aud Cx and Diffusion Rt Ext Cap



## Chapter 6: Discussion

In this study, we have validated a method to non-invasively assess the extent of cerebrovascular deficits in young adults male rats following traumatic brain injury. The method employed hypercapnia as a vasodilatory stimulus, which resulted in a robust increase in CBF across brain regions in healthy animals. Deficits in resting CBF as well as CBF during hypercapnia were observed in the auditory cortex ipsilateral to the side of impact. These results support and expand upon recent work of Long et al., who demonstrated that rats subjected to CCI exhibited increased resting CBF on day 2, decreased CBF day 7, and nearly normalized CBF by day 14 within the impact core, while the perilesional cortex showed diminished CBF days 2, and 7, and returned toward normal by day 14 (81). Our observations of persistent CBF reductions in the auditory cortex following FPI are most similar to the observations of the perilesional cortex of the CCI model since damage in the auditory cortex was not a result of direct impact, as the craniotomy was more medial and superior. Indeed, the auditory cortex also showed a significant increase in reactive astrocytes and microglia by GFAP and Iba-1 immunostaining respectively, suggesting response to focal injury located distal to the site of impact, supporting MRI findings.

This effect is consistent with cases of human TBI, in which contusions and lacerations are commonly distributed where the surface of the brain contacts the bony protuberances of the skull (44) and where neighboring heterogeneous structures within the brain act as a fulcrum (13). Interestingly, within the ipsilateral auditory cortex, CBF during hypercapnia trended downward through time points, reaching a statistically significant attenuated level by day 30.

Examination of the percent CBF change in response to hypercapnia, our study showed a general trend for early reduction in the cerebrovascular response in the injured auditory cortex 24 hours after injury, followed by a slight increase on day 7, and return toward baseline by day 30. When regional CVR was normalized to the contralateral ROI, CVR showed a considerable range in the auditory cortex on days 7 and 30, which may explain the failure to reach statistically significant levels. Potential contributing factors may include the heterogeneous response to injury among individual animals. Additionally, it is important to remember that CVR itself is a measure composed of two values in this study; therefore differences in either resting CBF, whether related to effects of injury or anesthesia, or differences in CBF with hypercapnia, which may be independently affected by injury or anesthesia, may contribute to the observed variation. Although anesthesia was regulated in this study by maintaining respiratory rate (RR) at 55 breaths per minute ( $\pm 5$ ), fluctuations in RR, as well as the level of end-tidal CO<sub>2</sub> may have contributed to differences in basal CBF and response to hypercapnia. Future studies are warranted to examine the interplay of these factors following TBI.

The second aim of this project was to assess the effect of sildenafil as a cytoprotective treatment. Interestingly, neither the resting CBF deficits nor that observed with hypercapnia in the right auditory cortex in saline treated animals were observed for animals that received sildenafil treatment. Rather, animals that received sildenafil treatment did not demonstrate deficits in any ROI at any time point. In direct analysis of the effect of treatment, sildenafil did not show a statistically significant main effect on

either resting CBF or CBF during hypercapnia in the right auditory cortex, despite trends of ameliorating deficits. Nevertheless, these are promising results lending in favor of therapeutic interventions which potentiate nitric oxide signaling. Similarly, sildenafil appeared to improve neurologic outcome as assessed by the NSS and NSS-R, though these trends were not found to be statistically significant.

One limitation of this study is the surprising subtlety of functional deficits after injury, which limited the ability to detect treatment effect. Peak neurologic dysfunction was observed on day 1, which by the NSS was equal to less than a one point deficit. Conversely, injured animals with saline injection showed a 3 point deficit day 1 after FPI by the NSS-R, with a return to baseline showing less variability than the NSS. In this study, the NSS-R appeared to be more sensitive in detecting deficits, and is therefore recommended for use in future studies.

Open field testing revealed no differences in total distance traveled among groups, suggesting that gross motor function was not adversely affected following injury. Injured groups, with saline or sildenafil treatment, spent more time in the center of the open field. Traditionally, this would suggest less anxiety-like behavior, which is the opposite effect we expected to occur with injury. As shown in the box and whiskers plot, injured animals showed greater variability in center time, which may reflect the spectrum of behavior outcomes observed in human TBI. No effect of sildenafil was observed for open field testing. Results from rotorod testing are inconclusive due to the limited number of animals tested due to equipment malfunction.

Water maze testing showed animals in all groups were able to quickly learn to find the platform. By the second day of training, the animals were able to rapidly find the

platform by the second trial, with a trend for equal performance among all groups through trials 2-5. In examining trial one across the three days of training and on the test day when the platform was moved, no clear trends were observed, suggesting intact hippocampal-dependent learning and memory. This is consistent with imaging data, as resting CBF, CBF with hypercapnia, and CVR were not altered for either left or right hippocampus following injury.

While this study is the first to assess the effect of sildenafil after fluid percussion injury, the potential utility of this agent in restoring cerebrovascular function is supported by its success in ameliorating embolic stroke in rodent models (30; 76; 143), decreasing burden of beta-amyloid in mouse models of Alzheimer's Disease (99), and in improving cerebrovascular function in patients with pulmonary hypertension (103).

In comparing the success of pre-clinical and clinical studies, and in planning for future studies, it is important to keep in mind differences in pharmacokinetics of the drug of interest. Sildenafil has a plasma clearance of 48 ml/min/kg in the male rat, 13 ml/min/kg in the female rat, and 6.0 ml/min/kg in man. Each has a similar volume of distribution (1.0, 2.0, and 1.2 L/kg, respectively), yielding a half-life of less than 1 h in the male rat, 1.9 hr in the female rat, and 2.4 hr in man (130). Thus, sildenafil studies in male rats may benefit from *bid* or *tid* dosing regimens. Additionally, tadalafil, another FDA-approved phosphodiesterase-5 inhibitor, is also worth consideration in future studies given its longer half-life of 17.5 hr (38).



The third aim of this study was to investigate the relation of MR-based assessments of cerebrovascular injury with axonal injury by DTI. In the right auditory cortex, where resting CBF was decreased significantly on day 7 and 30, and CBF during hypercapnia was decreased day 30, there was a co-existing increase in MD days 1 and 30, and increase in RD days 1, 7, and 30. These findings suggest that concomitant to disrupted blood flow in this region, there existed altered microstructural integrity with disrupted myelin. Analysis of correlation of DTI scalars with resting CBF failed to identify any statistically significant correlation of either MD or RD, and no correlation was significant after correction for multiple comparisons. Interestingly, sildenafil reversed the day 1 increase in MD in the medial cortex.

The right external capsule, which demonstrated an increase in reactive astrocytes, microglia, and microvascular density after injury, was also assessed for microstructural deficits after injury by DTI. MD was increased on day 1, suggesting early alteration in microstructural integrity, an effect that was reversed with sildenafil treatment. FA was decreased at all time points in the lateral segment, indicating a change toward isotropic diffusion after injury. On day 1, this coincided with an increase in both RD and AD, suggesting early myelin and axonal damage, respectively. Sildenafil significantly decreased RD on day 1, suggesting attenuation of early myelin damage, and increased FA on day 30, suggesting restoration of anisotropic diffusion along axons. Unexpectedly, AD was decreased days 7 and 30, reflective of restricted diffusion perpendicular to axonal fibers, though the mechanism for these temporal changes remains unknown. Interestingly, days 7 and 30 also marked the period in which resting CBF was attenuated in the adjacent gray matter of the auditory cortex. However, no correlation was found

between resting CBF and AD among individual animals, suggesting that these findings exist independently.

In summary, sildenafil appears to reverse several microstructural alterations following TBI. In injured animals that received only saline injection, there was no established correlation between cerebrovascular function and microstructural alterations, implicating two separate pathophysiological mechanisms following injury. Thus, it is possible that sildenafil's effect ameliorating microstructural damage exists independently from its effect on cerebrovascular function. Further studies are indicated to gain insight into the relationship between compromised cerebrovascular function and microstructural abnormalities after injury, and to better understand how sildenafil alters the pathophysiological course of disease. One limitation of this study is that diffusion studies were not yet validated by histologic analysis of axonal injury, which may also provide further insight into sildenafil's effect on axonal injury. Histologic analysis of axonal injury using  $\beta$ -APP immunostaining is planned for future study using tissue from this cohort.

## CONCLUSION

This study presented a non-invasive method to assess spatiotemporal changes in cerebrovascular function *in-vivo* following FPI, which was validated through histologic assessment. Regional deficits in cerebrovascular function occurred in the same regions as those with increased astrogliosis and microglial activation. The CBF deficits at rest and during hypercapnia that were observed in injured animals were not seen for the injured group that received sildenafil treatment, though a statistically significant main effect of

treatment was not detected. Sildenafil treated animals also showed a trend toward ameliorated neurologic function following injury. Diffusion imaging revealed significant microstructural changes following injury, many of which were reversed with sildenafil treatment. However, correlation between CBF and DTI scalars could not be established. Further research is indicated to investigate the relationship between cerebrovascular function and axonal injury after TBI, and to understand the mechanism(s) by which sildenafil alters the pathophysiologic course of disease.

## Appendix I

### NEUROLOGIC SEVERITY SCORE (NSS)

	Points
Inability to exit from a circle (50 cm in diameter) when left in its center	
Within 30 min	1
Within 60 min	1
At >60 min	1
Loss of righting reflex	
For 20 min	1
For 40 min	1
For 60 min	1
Hemiplegia-inability of the rat to resist forced changes in position	1
Flexion of hindlimb when raised by the tail	1
Inability to walk straight when placed on the floor	1
Inability to move	1
Reflexes	
Startle reflex	1
Pinna reflex	1
Clinical grade	
Loss of seeking behavior	1
Prostration	1

## Limb Reflexes

### Loss of placing reflexes

Forelimbs left	1
Forelimbs right	1
Hindlimbs left	1
Hindlimbs right	1

## Functional tests

### Failure in beam balancing task (1 .5 cm wide)

For 20 s	1
For 40 s	1
For 60 s	1

### Failure in beam-walking task

8.5 cm wide	1
5.0 cm wide	1
2.5 cm wide	1

TOTAL POINTS	24
--------------	----

### **NEUROBEHAVIORAL SCALE**

Each category is scored on a scale of 0-4 with 0 being non-functional and 4 being normal.

Forelimb Flexion upon suspension by tail

Decrease in resistance to lateral pulsion

Circling behavior upon spontaneous ambulation

Ability to stand on an inclined plane

Open Field Activity/ Exploratory Behavior

TOTAL POINTS      20

### **NIH STROKE SEVERITY SCORE**

Based on observed deficits, a functional grade is assessed:

Grade 0: Normal rat

Grade 1: Lethargy

Grade 2: Clear signs of paresis in at least one limb but able to walk

Grade 3: Severe paresis/paralysis, unable to walk

Grade 4: Dead

## REFERENCES

1. Adams CW, Bruton CJ. 1989. The cerebral vasculature in dementia pugilistica. *J Neurol Neurosurg Psychiatry* 52:600-4
2. Alexopoulos GS, Meyers BS, Young RC, Campbell S, Silbersweig D, Charlson M. 1997. 'Vascular depression' hypothesis. *Arch Gen Psychiatry* 54:915-22
3. Andresen J, Shafi NI, Bryan RM, Jr. 2006. Endothelial influences on cerebrovascular tone. *J Appl Physiol* 100:318-27
4. Andriessen TM, Jacobs B, Vos PE. 2010. Clinical characteristics and pathophysiological mechanisms of focal and diffuse traumatic brain injury. *J Cell Mol Med* 14:2381-92
5. Arfanakis K, Haughton VM, Carew JD, Rogers BP, Dempsey RJ, Meyerand ME. 2002. Diffusion tensor MR imaging in diffuse axonal injury. *AJNR Am J Neuroradiol* 23:794-802
6. Bailey DM, Jones DW, Sinnott A, Brugniaux JV, New KJ, et al. 2013. Impaired cerebral haemodynamic function associated with chronic traumatic brain injury in professional boxers. *Clin Sci (Lond)* 124:177-89
7. Bakker SL, de Leeuw FE, de Groot JC, Hofman A, Koudstaal PJ, Breteler MM. 1999. Cerebral vasomotor reactivity and cerebral white matter lesions in the elderly. *Neurology* 52:578-83
8. Baranova AI, Wei EP, Ueda Y, Sholley MM, Kontos HA, Povlishock JT. 2008. Cerebral vascular responsiveness after experimental traumatic brain injury: the beneficial effects of delayed hypothermia combined with superoxide dismutase administration. *J Neurosurg* 109:502-9
9. Barbier EL, Silva AC, Kim SG, Koretsky AP. 2001. Perfusion imaging using dynamic arterial spin labeling (DASL). *Magn Reson Med* 45:1021-9
10. Bartnik-Olson BL, Holshouser B, Wang H, Grube M, Tong K, et al. 2014. Impaired neurovascular unit function contributes to persistent symptoms after concussion: a pilot study. *J Neurotrauma* 31:1497-506
11. Bazarian JJ, Zhong J, Blyth B, Zhu T, Kavcic V, Peterson D. 2007. Diffusion tensor imaging detects clinically important axonal damage after mild traumatic brain injury: a pilot study. *J Neurotrauma* 24:1447-59
12. Bederson JB, Bartkowski HM, Moon K, Halks-Miller M, Nishimura MC, et al. 1986. Nuclear magnetic resonance imaging and spectroscopy in experimental brain edema in a rat model. *J Neurosurg* 64:795-802
13. Bigler ED, Maxwell WL. 2011. Neuroimaging and neuropathology of TBI. *NeuroRehabilitation* 28:63-74
14. Bitner BR, Brink DC, Mathew LC, Pautler RG, Robertson CS. 2010. Impact of arginase II on CBF in experimental cortical impact injury in mice using MRI. *J Cereb Blood Flow Metab* 30:1105-9
15. Bokkers RP, Hernandez DA, Merino JG, Mirasol RV, van Osch MJ, et al. 2012. Whole-brain arterial spin labeling perfusion MRI in patients with acute stroke. *Stroke* 43:1290-4

16. Bokkers RP, van Osch MJ, Klijn CJ, Kappelle LJ, Hendrikse J. 2011. Cerebrovascular reactivity within perfusion territories in patients with an internal carotid artery occlusion. *J Neurol Neurosurg Psychiatry* 82:1011-6
17. Bokkers RP, van Osch MJ, van der Worp HB, de Borst GJ, Mali WP, Hendrikse J. 2010. Symptomatic carotid artery stenosis: impairment of cerebral autoregulation measured at the brain tissue level with arterial spin-labeling MR imaging. *Radiology* 256:201-8
18. Bonne O, Gilboa A, Louzoun Y, Kempf-Sherf O, Katz M, et al. 2003. Cerebral blood flow in chronic symptomatic mild traumatic brain injury. *Psychiatry Res* 124:141-52
19. Borgens RB, Liu-Snyder P. 2012. Understanding secondary injury. *Q Rev Biol* 87:89-127
20. Carroll LJ, Cassidy JD, Holm L, Kraus J, Coronado VG. 2004. Methodological issues and research recommendations for mild traumatic brain injury: the WHO Collaborating Centre Task Force on Mild Traumatic Brain Injury. *J Rehabil Med*:113-25
21. Chen SH, Wang JJ, Chen CH, Chang HK, Lin MT, et al. 2013. Umbilical cord blood-derived CD34+ cells improve outcomes of traumatic brain injury in rats by stimulating angiogenesis and neurogenesis. *Cell Transplant*
22. Cohen Z, Bonvento G, Lacombe P, Hamel E. 1996. Serotonin in the regulation of brain microcirculation. *Prog Neurobiol* 50:335-62
23. Cole JT, Yarnell A, Kean WS, Gold E, Lewis B, et al. 2011. Craniotomy: true sham for traumatic brain injury, or a sham of a sham? *J Neurotrauma* 28:359-69
24. Coronado VG, Xu L, Basavaraju SV, McGuire LC, Wald MM, et al. 2011. Surveillance for traumatic brain injury-related deaths--United States, 1997-2007. *MMWR Surveill Summ* 60:1-32
25. Deroulers C, Ameisen D, Badoual M, Gerin C, Granier A, Lartaud M. 2013. Analyzing huge pathology images with open source software. *Diagn Pathol* 8:92
26. Detre JA, Rao H, Wang DJ, Chen YF, Wang Z. 2012. Applications of arterial spin labeled MRI in the brain. *J Magn Reson Imaging* 35:1026-37
27. DeWitt DS, Prough DS. 2003. Traumatic cerebral vascular injury: the effects of concussive brain injury on the cerebral vasculature. *J Neurotrauma* 20:795-825
28. Diaz-Arrastia R, Kochanek PM, Bergold P, Kenney K, Marx CE, et al. 2014. Pharmacotherapy of traumatic brain injury: state of the science and the road forward: report of the Department of Defense Neurotrauma Pharmacology Workgroup. *J Neurotrauma* 31:135-58
29. Dietrich WD, Alonso O, Busto R, Prado R, Dewanjee S, et al. 1996. Widespread hemodynamic depression and focal platelet accumulation after fluid percussion brain injury: a double-label autoradiographic study in rats. *J Cereb Blood Flow Metab* 16:481-9
30. Ding G, Jiang Q, Li L, Zhang L, Zhang ZG, et al. 2008. Magnetic resonance imaging investigation of axonal remodeling and angiogenesis after embolic stroke in sildenafil-treated rats. *J Cereb Blood Flow Metab* 28:1440-8



31. Dufouil C, de Kersaint-Gilly A, Besancon V, Levy C, Auffray E, et al. 2001. Longitudinal study of blood pressure and white matter hyperintensities: the EVA MRI Cohort. *Neurology* 56:921-6
32. Dutton RP, Prior K, Cohen R, Wade C, Sewell J, et al. 2011. Diagnosing mild traumatic brain injury: where are we now? *J Trauma* 70:554-9
33. Fathi AR, Bakhtian KD, Pluta RM. 2011. The role of nitric oxide donors in treating cerebral vasospasm after subarachnoid hemorrhage. *Acta Neurochir Suppl* 110:93-7
34. Faul M XL, Wald MM, Coronado VG. 2010. Traumatic Brain Injury in the United States: Emergency Department Visits, Hospitalizations and Deaths 2002–2006. ed. NCFIPaC Centers for Disease Control and Prevention. Atlanta, GA
35. Faul M, Xu L, Wald MM, Coronado VG. 2010. Traumatic Brain Injury in the United States: Emergency Department Visits, Hospitalizations and Deaths 2002–2006. Atlanta (GA): National Center for Injury Prevention and Control, Centers for Disease Control and Prevention
36. Finkelstein E CP, Miller TR. 2006. The incidence and economic burden of injuries in the United States. Oxford, New York: Oxford University Press
37. Forbes ML, Hendrich KS, Kochanek PM, Williams DS, Schiding JK, et al. 1997. Assessment of cerebral blood flow and CO<sub>2</sub> reactivity after controlled cortical impact by perfusion magnetic resonance imaging using arterial spin-labeling in rats. *J Cereb Blood Flow Metab* 17:865-74
38. Forgue ST, Patterson BE, Bedding AW, Payne CD, Phillips DL, et al. 2006. Tadalafil pharmacokinetics in healthy subjects. *Br J Clin Pharmacol* 61:280-8
39. Gavett BE, Stern RA, McKee AC. 2011. Chronic traumatic encephalopathy: a potential late effect of sport-related concussive and subconcussive head trauma. *Clin Sports Med* 30:179-88, xi
40. Golding EM. 2002. Sequelae following traumatic brain injury. The cerebrovascular perspective. *Brain Res Brain Res Rev* 38:377-88
41. Golding EM, Robertson CS, Bryan RM, Jr. 2000. L-arginine partially restores the diminished CO<sub>2</sub> reactivity after mild controlled cortical impact injury in the adult rat. *J Cereb Blood Flow Metab* 20:820-8
42. Goldstein LE, Fisher AM, Tagge CA, Zhang XL, Velisek L, et al. 2012. Chronic traumatic encephalopathy in blast-exposed military veterans and a blast neurotrauma mouse model. *Sci Transl Med* 4:134ra60
43. Goode SD, Krishan S, Alexakis C, Mahajan R, Auer DP. 2009. Precision of cerebrovascular reactivity assessment with use of different quantification methods for hypercapnia functional MR imaging. *AJNR Am J Neuroradiol* 30:972-7
44. Graham DI, Adams JH, Nicoll JA, Maxwell WL, Gennarelli TA. 1995. The nature, distribution and causes of traumatic brain injury. *Brain Pathol* 5:397-406
45. Grubb RL, Jr., Raichle ME, Eichling JO, Ter-Pogossian MM. 1974. The effects of changes in PaCO<sub>2</sub> on cerebral blood volume, blood flow, and vascular mean transit time. *Stroke* 5:630-9
46. Haacke EM, Mittal S, Wu Z, Neelavalli J, Cheng YC. 2009. Susceptibility-weighted imaging: technical aspects and clinical applications, part 1. *AJNR Am J Neuroradiol* 30:19-30

47. Hamel E. 1985. Perivascular nerves and the regulation of cerebrovascular tone. *J Appl Physiol* 100:1059-64
48. Hartikainen KM, Waljas M, Isoviita T, Dastidar P, Liimatainen S, et al. 2010. Persistent symptoms in mild to moderate traumatic brain injury associated with executive dysfunction. *J Clin Exp Neuropsychol* 32:767-74
49. Hayward NM, Immonen R, Tuunanen PI, Nodde-Ekane XE, Grohn O, Pitkanen A. 2010. Association of chronic vascular changes with functional outcome after traumatic brain injury in rats. *J Neurotrauma* 27:2203-19
50. Hayward NM, Tuunanen PI, Immonen R, Nodde-Ekane XE, Pitkanen A, Grohn O. 2011. Magnetic resonance imaging of regional hemodynamic and cerebrovascular recovery after lateral fluid-percussion brain injury in rats. *J Cereb Blood Flow Metab* 31:166-77
51. Hendrich KS, Kochanek PM, Williams DS, Schiding JK, Marion DW, Ho C. 1999. Early perfusion after controlled cortical impact in rats: quantification by arterial spin-labeled MRI and the influence of spin-lattice relaxation time heterogeneity. *Magn Reson Med* 42:673-81
52. Hoge RD, Atkinson J, Gill B, Crelier GR, Marrett S, Pike GB. 1999. Investigation of BOLD signal dependence on cerebral blood flow and oxygen consumption: the deoxyhemoglobin dilution model. *Magn Reson Med* 42:849-63
53. Hsu SM, Raine L, Fanger H. 1981. Use of avidin-biotin-peroxidase complex (ABC) in immunoperoxidase techniques: a comparison between ABC and unlabeled antibody (PAP) procedures. *J Histochem Cytochem* 29:577-80
54. Huang YL, Kuo YS, Tseng YC, Chen DY, Chiu WT, Chen CJ. 2015. Susceptibility-weighted MRI in mild traumatic brain injury. *Neurology* 84:580-5
55. Hunter JV, Wilde EA, Tong KA, Holshouser BA. 2012. Emerging imaging tools for use with traumatic brain injury research. *J Neurotrauma* 29:654-71
56. Hyder AA, Wunderlich CA, Puvanachandra P, Gururaj G, Kobusingye OC. 2007. The impact of traumatic brain injuries: a global perspective. *NeuroRehabilitation* 22:341-53
57. Iadecola C. 2013. The pathobiology of vascular dementia. *Neuron* 80:844-66
58. Isaka Y, Okamoto M, Ashida K, Imaizumi M. 1994. Decreased cerebrovascular dilatory capacity in subjects with asymptomatic periventricular hyperintensities. *Stroke* 25:375-81
59. Jefferson AL, Tate DF, Poppas A, Brickman AM, Paul RH, et al. 2007. Lower cardiac output is associated with greater white matter hyperintensities in older adults with cardiovascular disease. *J Am Geriatr Soc* 55:1044-8
60. Kassner A, Roberts TP. 2004. Beyond perfusion: cerebral vascular reactivity and assessment of microvascular permeability. *Top Magn Reson Imaging* 15:58-65
61. Kenney K, Amyot F, Haber M, Pronger A, Bogoslovsky T, et al. 2016. Cerebral Vascular Injury in Traumatic Brain Injury. *Exp Neurol* 275 Pt 3:353-66
62. Kety SS, Schmidt CF. 1948. The Effects of Altered Arterial Tensions of Carbon Dioxide and Oxygen on Cerebral Blood Flow and Cerebral Oxygen Consumption of Normal Young Men. *J Clin Invest* 27:484-92
63. Khan M, Im YB, Shunmugavel A, Gilg AG, Dhindsa RK, et al. 2009. Administration of S-nitrosoglutathione after traumatic brain injury protects the

- neurovascular unit and reduces secondary injury in a rat model of controlled cortical impact. *J Neuroinflammation* 6:32
64. Kim J, Whyte J, Patel S, Avants B, Europa E, et al. 2010. Resting cerebral blood flow alterations in chronic traumatic brain injury: an arterial spin labeling perfusion fMRI study. *J Neurotrauma* 27:1399-411
  65. Kochanek PM, Hendrich KS, Dixon CE, Schiding JK, Williams DS, Ho C. 2002. Cerebral blood flow at one year after controlled cortical impact in rats: assessment by magnetic resonance imaging. *J Neurotrauma* 19:1029-37
  66. Kou Z, Wu Z, Tong KA, Holshouser B, Benson RR, et al. 2010. The role of advanced MR imaging findings as biomarkers of traumatic brain injury. *J Head Trauma Rehabil* 25:267-82
  67. Kraus MF, Susmaras T, Caughlin BP, Walker CJ, Sweeney JA, Little DM. 2007. White matter integrity and cognition in chronic traumatic brain injury: a diffusion tensor imaging study. *Brain* 130:2508-19
  68. Krejza J, Rudzinski W, Arkuszewski M, Onuoha O, Melhem ER. 2013. Cerebrovascular reactivity across the menstrual cycle in young healthy women. *Neuroradiol J* 26:413-9
  69. Kumar A, Loane DJ. 2012. Neuroinflammation after traumatic brain injury: Opportunities for therapeutic intervention. *Brain Behav Immun*
  70. Kumar R, Gupta RK, Husain M, Chaudhry C, Srivastava A, et al. 2009. Comparative evaluation of corpus callosum DTI metrics in acute mild and moderate traumatic brain injury: its correlation with neuropsychometric tests. *Brain Inj* 23:675-85
  71. Kurland DB, Tosun C, Pampori A, Karimy JK, Caffes NM, et al. 2013. Glibenclamide for the treatment of acute CNS injury. *Pharmaceuticals (Basel)* 6:1287-303
  72. Laitinen T, Sierra A, Bolkvadze T, Pitkanen A, Grohn O. 2015. Diffusion tensor imaging detects chronic microstructural changes in white and gray matter after traumatic brain injury in rat. *Front Neurosci* 9:128
  73. Len TK, Neary JP, Asmundson GJ, Goodman DG, Bjornson B, Bhambhani YN. 2011. Cerebrovascular reactivity impairment after sport-induced concussion. *Med Sci Sports Exerc* 43:2241-8
  74. Leoni RF, Mazzetto-Betti KC, Silva AC, Dos Santos AC, de Araujo DB, et al. 2012. Assessing Cerebrovascular Reactivity in Carotid Steno-Occlusive Disease Using MRI BOLD and ASL Techniques. *Radiol Res Pract* 2012:268483
  75. Lewelt W, Jenkins LW, Miller JD. 1980. Autoregulation of cerebral blood flow after experimental fluid percussion injury of the brain. *J Neurosurg* 53:500-11
  76. Li L, Jiang Q, Zhang L, Ding G, Gang Zhang Z, et al. 2007. Angiogenesis and improved cerebral blood flow in the ischemic boundary area detected by MRI after administration of sildenafil to rats with embolic stroke. *Brain Res* 1132:185-92
  77. Li S, Wei M, Zhou Z, Wang B, Zhao X, Zhang J. 2012. SDF-1alpha induces angiogenesis after traumatic brain injury. *Brain Res* 1444:76-86

78. Lin B, Ginsberg MD, Zhao W, Alonso OF, Belayev L, Busto R. 2001. Quantitative analysis of microvascular alterations in traumatic brain injury by endothelial barrier antigen immunohistochemistry. *J Neurotrauma* 18:389-97
79. Lin L, Xue Y, Duan Q, Sun B, Lin H, et al. 2015. Microstructural White Matter Abnormalities and Cognitive Dysfunction in Subcortical Ischemic Vascular Disease: an Atlas-Based Diffusion Tensor Analysis Study. *J Mol Neurosci* 56:363-70
80. Loane DJ, Pocivavsek A, Moussa CE, Thompson R, Matsuoka Y, et al. 2009. Amyloid precursor protein secretases as therapeutic targets for traumatic brain injury. *Nat Med* 15:377-9
81. Long JA, Watts LT, Li W, Shen Q, Muir ER, et al. 2015. The effects of perturbed cerebral blood flow and cerebrovascular reactivity on structural MRI and behavioral readouts in mild traumatic brain injury. *J Cereb Blood Flow Metab* 35:1852-61
82. Longstreth WT, Jr., Manolio TA, Arnold A, Burke GL, Bryan N, et al. 1996. Clinical correlates of white matter findings on cranial magnetic resonance imaging of 3301 elderly people. The Cardiovascular Health Study. *Stroke* 27:1274-82
83. Lu D, Mahmood A, Zhang R, Copp M. 2003. Upregulation of neurogenesis and reduction in functional deficits following administration of DETA/NONOate, a nitric oxide donor, after traumatic brain injury in rats. *J Neurosurg* 99:351-61
84. MacIntosh BJ, Lindsay AC, Kyntireas I, Kuker W, Gunther M, et al. 2010. Multiple inflow pulsed arterial spin-labeling reveals delays in the arterial arrival time in minor stroke and transient ischemic attack. *AJNR Am J Neuroradiol* 31:1892-4
85. Masel BE, DeWitt DS. 2010. Traumatic brain injury: a disease process, not an event. *J Neurotrauma* 27:1529-40
86. Mayer AR, Ling J, Mannell MV, Gasparovic C, Phillips JP, et al. 2010. A prospective diffusion tensor imaging study in mild traumatic brain injury. *Neurology* 74:643-50
87. McKee AC, Cairns NJ, Dickson DW, Folkerth RD, Keene CD, et al. 2016. The first NINDS/NIBIB consensus meeting to define neuropathological criteria for the diagnosis of chronic traumatic encephalopathy. *Acta Neuropathol* 131:75-86
88. Miles L, Grossman RI, Johnson G, Babb JS, Diller L, Inglese M. 2008. Short-term DTI predictors of cognitive dysfunction in mild traumatic brain injury. *Brain Inj* 22:115-22
89. Novak V, Last D, Alsop DC, Abduljalil AM, Hu K, et al. 2006. Cerebral blood flow velocity and periventricular white matter hyperintensities in type 2 diabetes. *Diabetes Care* 29:1529-34
90. Ogawa S, Tank DW, Menon R, Ellermann JM, Kim SG, et al. 1992. Intrinsic signal changes accompanying sensory stimulation: functional brain mapping with magnetic resonance imaging. *Proc Natl Acad Sci U S A* 89:5951-5
91. Omalu B, Bailes J, Hamilton RL, Kamboh MI, Hammers J, et al. 2011. Emerging histomorphologic phenotypes of chronic traumatic encephalopathy in American athletes. *Neurosurgery* 69:173-83; discussion 83

92. Oppenheimer DR. 1968. Microscopic lesions in the brain following head injury. *J Neurol Neurosurg Psychiatry* 31:299-306
93. Pantoni L, Garcia JH, Gutierrez JA. 1996. Cerebral white matter is highly vulnerable to ischemia. *Stroke* 27:1641-6; discussion 7
94. Park E, Bell JD, Siddiq IP, Baker AJ. 2009. An analysis of regional microvascular loss and recovery following two grades of fluid percussion trauma: a role for hypoxia-inducible factors in traumatic brain injury. *J Cereb Blood Flow Metab* 29:575-84
95. Pasi M, Poggesi A, Salvadori E, Diciotti S, Ciolli L, et al. 2015. White matter microstructural damage and depressive symptoms in patients with mild cognitive impairment and cerebral small vessel disease: the VMCI-Tuscany Study. *Int J Geriatr Psychiatry*
96. Pierpaoli C, Walker L, Irfanoglu MO, Barnett A, Basser P, et al. TORTOISE: an integrated software package for processing of diffusion MRI data. *Proc. ISMRM 18th annual meeting, Stockholm, Sweden, 2010:*
97. Pollock JM, Deibler AR, Burdette JH, Kraft RA, Tan H, et al. 2008. Migraine associated cerebral hyperperfusion with arterial spin-labeled MR imaging. *AJNR Am J Neuroradiol* 29:1494-7
98. Pollock JM, Deibler AR, West TG, Burdette JH, Kraft RA, Maldjian JA. 2008. Arterial spin-labeled magnetic resonance imaging in hyperperfused seizure focus: a case report. *J Comput Assist Tomogr* 32:291-2
99. Puzzo D, Staniszewski A, Deng SX, Privitera L, Leznik E, et al. 2009. Phosphodiesterase 5 inhibition improves synaptic function, memory, and amyloid-beta load in an Alzheimer's disease mouse model. *J Neurosci* 29:8075-86
100. Rodriguez-Baeza A, Reina-de la Torre F, Poca A, Marti M, Garnacho A. 2003. Morphological features in human cortical brain microvessels after head injury: a three-dimensional and immunocytochemical study. *Anat Rec A Discov Mol Cell Evol Biol* 273:583-93
101. Ropper AH, Gorson KC. 2007. Clinical practice. Concussion. *N Engl J Med* 356:166-72
102. Rosenberg GA. 2009. Inflammation and white matter damage in vascular cognitive impairment. *Stroke* 40:S20-3
103. Rosengarten B, Schermuly RT, Voswinckel R, Kohstall MG, Olschewski H, et al. 2006. Sildenafil improves dynamic vascular function in the brain: studies in patients with pulmonary hypertension. *Cerebrovasc Dis* 21:194-200
104. Roy CS, Sherrington CS. 1890. On the Regulation of the Blood-supply of the Brain. *J Physiol* 11:85-158 17
105. Ruff RM, Crouch JA, Troster AI, Marshall LF, Buchsbaum MS, et al. 1994. Selected cases of poor outcome following a minor brain trauma: comparing neuropsychological and positron emission tomography assessment. *Brain Inj* 8:297-308
106. Saatman KE, Duhaime AC, Bullock R, Maas AI, Valadka A, et al. 2008. Classification of traumatic brain injury for targeted therapies. *J Neurotrauma* 25:719-38

107. Sangiorgi S, De Benedictis A, Protasoni M, Manelli A, Reguzzoni M, et al. 2013. Early-stage microvascular alterations of a new model of controlled cortical traumatic brain injury: 3D morphological analysis using scanning electron microscopy and corrosion casting. *J Neurosurg* 118:763-74
108. Scherer MR, Schubert MC. 2009. Traumatic brain injury and vestibular pathology as a comorbidity after blast exposure. *Phys Ther* 89:980-92
109. Schindelin J, Arganda-Carreras I, Frise E, Kaynig V, Longair M, et al. 2012. Fiji: an open-source platform for biological-image analysis. *Nat Methods* 9:676-82
110. Shenton ME, Hamoda HM, Schneiderman JS, Bouix S, Pasternak O, et al. 2012. A review of magnetic resonance imaging and diffusion tensor imaging findings in mild traumatic brain injury. *Brain Imaging Behav*
111. Shlosberg D, Benifla M, Kaufer D, Friedman A. 2010. Blood-brain barrier breakdown as a therapeutic target in traumatic brain injury. *Nat Rev Neurol* 6:393-403
112. Sicard KM, Duong TQ. 2005. Effects of hypoxia, hyperoxia, and hypercapnia on baseline and stimulus-evoked BOLD, CBF, and CMRO<sub>2</sub> in spontaneously breathing animals. *Neuroimage* 25:850-8
113. Sidaros A, Engberg AW, Sidaros K, Liptrot MG, Herning M, et al. 2008. Diffusion tensor imaging during recovery from severe traumatic brain injury and relation to clinical outcome: a longitudinal study. *Brain* 131:559-72
114. Silva AC, Kim SG. 1999. Pseudo-continuous arterial spin labeling technique for measuring CBF dynamics with high temporal resolution. *Magn Reson Med* 42:425-9
115. Sivanandam TM, Thakur MK. 2012. Traumatic brain injury: A risk factor for Alzheimer's disease. *Neurosci Biobehav Rev*
116. Stein SC, Chen XH, Sinson GP, Smith DH. 2002. Intravascular coagulation: a major secondary insult in nonfatal traumatic brain injury. *J Neurosurg* 97:1373-7
117. Stern RA, Riley DO, Daneshvar DH, Nowinski CJ, Cantu RC, McKee AC. 2011. Long-term consequences of repetitive brain trauma: chronic traumatic encephalopathy. *Pm R* 3:S460-7
118. Stone JR, Singleton RH, Povlishock JT. 2000. Antibodies to the C-terminus of the beta-amyloid precursor protein (APP): a site specific marker for the detection of traumatic axonal injury. *Brain Res* 871:288-302
119. Tan CO, Meehan WP, 3rd, Iverson GL, Taylor JA. 2014. Cerebrovascular regulation, exercise, and mild traumatic brain injury. *Neurology* 83:1665-72
120. Taylor WD, Aizenstein HJ, Alexopoulos GS. 2013. The vascular depression hypothesis: mechanisms linking vascular disease with depression. *Mol Psychiatry* 18:963-74
121. Terpolilli NA, Kim SW, Thal SC, Kuebler WM, Plesnila N. 2013. Inhaled nitric oxide reduces secondary brain damage after traumatic brain injury in mice. *J Cereb Blood Flow Metab* 33:311-8
122. Thau-Zuchman O, Shohami E, Alexandrovich AG, Leker RR. 2012. Combination of vascular endothelial and fibroblast growth factor 2 for induction of neurogenesis and angiogenesis after traumatic brain injury. *J Mol Neurosci* 47:166-72

123. Thomas AJ, Perry R, Barber R, Kalaria RN, O'Brien JT. 2002. Pathologies and pathological mechanisms for white matter hyperintensities in depression. *Ann N Y Acad Sci* 977:333-9
124. Thompson HJ, Lifshitz J, Marklund N, Grady MS, Graham DI, et al. 2005. Lateral fluid percussion brain injury: a 15-year review and evaluation. *J Neurotrauma* 22:42-75
125. Tomlinson BE. 1970. Brain-stem lesions after head injury. *J Clin Pathol Suppl (R Coll Pathol)* 4:154-65
126. Tong KA, Ashwal S, Holshouser BA, Nickerson JP, Wall CJ, et al. 2004. Diffuse axonal injury in children: clinical correlation with hemorrhagic lesions. *Ann Neurol* 56:36-50
127. Tong KA, Ashwal S, Holshouser BA, Shutter LA, Herigault G, et al. 2003. Hemorrhagic shearing lesions in children and adolescents with posttraumatic diffuse axonal injury: improved detection and initial results. *Radiology* 227:332-9
128. Van Boven RW, Harrington GS, Hackney DB, Ebel A, Gauger G, et al. 2009. Advances in neuroimaging of traumatic brain injury and posttraumatic stress disorder. *J Rehabil Res Dev* 46:717-57
129. Vink R, Nimmo AJ. 2009. Multifunctional drugs for head injury. *Neurotherapeutics* 6:28-42
130. Walker DK, Ackland MJ, James GC, Muirhead GJ, Rance DJ, et al. 1999. Pharmacokinetics and metabolism of sildenafil in mouse, rat, rabbit, dog and man. *Xenobiotica* 29:297-310
131. Wang B, Sun L, Tian Y, Li Z, Wei H, et al. 2012. Effects of atorvastatin in the regulation of circulating EPCs and angiogenesis in traumatic brain injury in rats. *J Neurol Sci* 319:117-23
132. Wei EP, Hamm RJ, Baranova AI, Povlishock JT. 2009. The long-term microvascular and behavioral consequences of experimental traumatic brain injury after hypothermic intervention. *J Neurotrauma* 26:527-37
133. Wilk JE, Thomas JL, McGurk DM, Riviere LA, Castro CA, Hoge CW. 2010. Mild traumatic brain injury (concussion) during combat: lack of association of blast mechanism with persistent postconcussive symptoms. *The Journal of head trauma rehabilitation* 25:9-14
134. Xing G, Barry ES, Benford B, Grunberg NE, Li H, et al. 2013. Impact of repeated stress on traumatic brain injury-induced mitochondrial electron transport chain expression and behavioral responses in rats. *Front Neurol* 4:196
135. Xiong Y, Mahmood A, Chopp M. 2010. Angiogenesis, neurogenesis and brain recovery of function following injury. *Curr Opin Investig Drugs* 11:298-308
136. Xiong Y, Zhang Y, Mahmood A, Meng Y, Qu C, Chopp M. 2011. Erythropoietin Mediates Neurobehavioral Recovery and Neurovascular Remodeling Following Traumatic Brain Injury in Rats by Increasing Expression of Vascular Endothelial Growth Factor. *Transl Stroke Res* 2:619-32
137. Yamakami I, McIntosh TK. 1989. Effects of traumatic brain injury on regional cerebral blood flow in rats as measured with radiolabeled microspheres. *J Cereb Blood Flow Metab* 9:117-24

138. Yarnell AM, Barry ES, Mountney A, Shear D, Tortella F, Grunberg NE. 2016. The revised neurobehavioral severity scale (NSS-R) for rodents. *Current Protocols in Neuroscience*
139. Yezhuvath US, Lewis-Amezcu K, Varghese R, Xiao G, Lu H. 2009. On the assessment of cerebrovascular reactivity using hypercapnia BOLD MRI. *NMR Biomed* 22:779-86
140. Ylikoski A, Erkinjuntti T, Raininko R, Sarna S, Sulkava R, Tilvis R. 1995. White matter hyperintensities on MRI in the neurologically nondiseased elderly. Analysis of cohorts of consecutive subjects aged 55 to 85 years living at home. *Stroke* 26:1171-7
141. Yuan XQ, Prough DS, Smith TL, Dewitt DS. 1988. The effects of traumatic brain injury on regional cerebral blood flow in rats. *J Neurotrauma* 5:289-301
142. Zhang F, Sprague SM, Farrokhi F, Henry MN, Son MG, Vollmer DG. 2002. Reversal of attenuation of cerebrovascular reactivity to hypercapnia by a nitric oxide donor after controlled cortical impact in a rat model of traumatic brain injury. *J Neurosurg* 97:963-9
143. Zhang R, Wang Y, Zhang L, Zhang Z, Tsang W, et al. 2002. Sildenafil (Viagra) induces neurogenesis and promotes functional recovery after stroke in rats. *Stroke* 33:2675-80